Available online at www.sciencedirect.com
SCIENCE DIRECT®
ELSEVIER
Planetary and Space Science 54 (2006) 879–910
Planetary and Space Science
www.elsevier.com/locate/pss

Galileo dust data from the jovian system: 1997–1999

H. Krüger[a,*], D. Bindschadler[b], S.F. Dermott[c], A.L. Graps[d], E. Grün[e,f], B.A. Gustafson[c], D.P. Hamilton[g], M.S. Hanner[b], M. Horányi[h], J. Kissel[a], B.A. Lindblad[i], D. Linkert[e], G. Linkert[e], I. Mann[j], J.A.M. McDonnell[k], R. Moissl[a], G.E. Morfill[l], C. Polanskey[b], G. Schwehm[m], R. Srama[e], H.A. Zook[n,✠]

[a]Max-Planck-Institut für Sonnensystemforschung, 37191 Katlenburg-Lindau, Germany
[b]Jet Propulsion Laboratory, Pasadena, CA 91109, USA
[c]University of Florida, 211 SSRB, Campus, Gainesville, FL 32609, USA
[d]Istituto di Fisica dello Spazio Interplanetario, INAF-ARTOV, 00133 Roma, Italy
[e]Max-Planck-Institut für Kernphysik, 69029 Heidelberg, Germany
[f]Hawaii Institute of Geophysics and Planetology, Honolulu, HI 96822, USA
[g]University of Maryland, College Park, MD 20742-2421, USA
[h]Laboratory for Atmospheric and Space Physics, University of Colorado, Boulder, CO 80309, USA
[i]Lund Observatory, 221 Lund, Sweden
[j]Institut für Planetologie, Universität Münster, 48149 Münster, Germany
[k]Planetary and Space Science Research Institute, The Open University, Milton Keynes, MK7 6AA, UK
[l]Max-Planck-Institut für Extraterrestrische Physik, 85748 Garching, Germany
[m]ESTEC, 2200 AG Noordwijk, The Netherlands
[n]NASA Johnson Space Center, Houston, TX 77058, USA

Received 20 December 2005; received in revised form 10 April 2006; accepted 25 April 2006
Available online 27 June 2006

Abstract

The dust detector system on board the Galileo spacecraft recorded dust impacts in circumjovian space during the craft's orbital mission about Jupiter. This is the eighth in a series of papers dedicated to presenting Galileo and Ulysses dust data. We present data from the Galileo dust instrument for the period January 1997–December 1999 when the spacecraft completed 21 revolutions about Jupiter. In this time interval data were obtained as high resolution realtime science data or recorded data during 449 days (representing 41% of the entire period), or via memory readouts during the remaining times. Because the data transmission rate of the spacecraft was very low, the complete data set (i.e. all parameters measured by the instrument during impact of a dust particle) of only 3% (7625) of all particles detected could be transmitted to Earth; the other particles were only counted. Together with the data of 2883 particles detected during Galileo's interplanetary cruise and 5353 particles detected in the jovian system in 1996, complete data of 15 861 particles detected by the Galileo dust instrument from 1989 to 1999 are now available. The majority of the detected particles were tiny grains (about 10 nm in radius), most of them originating from Jupiter's innermost Galilean moon Io. They were detected throughout the jovian system and the highest impact rates exceeded $100\,\mathrm{min}^{-1}$ (C21 orbit; 01 July 1999). With the new data set the times of onset, cessation and a 180° shift in the impact direction of the grains measured during 19 Galileo orbits about Jupiter are well reproduced by simulated 9 nm particles charged up to a potential of +3 V, confirming earlier results obtained for only two Galileo orbits (Horányi, M., Grün, E., Heck, A., 1997. Modeling the Galileo dust measurements at Jupiter. Geophys. Res. Lett. 24, 2175–2178). Galileo has detected a large number of bigger particles mostly in the region between the Galilean moons. The average radius of 370 of these grains measured in the 1996–1999 period is about 2 μm (assuming spherical grains with density $1\,\mathrm{g\,cm}^{-3}$) and the size distribution rises steeply towards smaller grains. The biggest detected particles have a radius of about 10 μm.

Keywords: Interplanetary dust; Circumplanetary dust; Dust streams; Jupiter dust; Dust clouds

*Corresponding author.
E-mail address: krueger@mps.mpg.de (H. Krüger).
✠Deceased 2001.

0032-0633/$ - see front matter
doi:10.1016/j.pss.2006.04.010

1. Introduction

The Galileo spacecraft was the first artificial satellite orbiting Jupiter. Galileo had a highly sensitive impact ionization dust detector on board which was identical with the dust detector of the Ulysses spacecraft (Grün et al., 1992a,b, Grün et al., 1995c). Dust data from both spacecraft were used for the analysis of e.g. the interplanetary dust complex, dust related to asteroids and comets, interstellar dust grains sweeping through the solar system, and various dust phenomena in the environment of Jupiter. Here we recall only publications which are related to dust in the Jupiter system. References to other works can be found in Krüger et al., (1999a,c). A comprehensive summary of the investigation of dust in the jovian system was given by Krüger et al. (2004).

Ulysses discovered streams of dust particles emanating from the jovian system (Grün et al., 1993) which were later confirmed by Galileo (Grün et al., 1996a,b). At least four dust populations were identified in the Jupiter system (Grün et al., 1997, 1998): (i) Streams of dust particles with high and variable impact rates throughout Jupiter's magnetosphere. The particles are about 10 nm in diameter (Zook et al., 1996) and they mostly originate from the innermost Galilean moon Io (Graps et al., 2000). Because of their small sizes the charged grains strongly interact with Jupiter's magnetosphere (Horányi et al., 1997; Grün et al., 1998; Heck, 1998). The dust streams served as a monitor of Io's volcanic plume activity (Krüger et al., 2003a) and as probes of the Io plasma torus (Krüger et al., 2003b). Dust charging mechanisms in Io's plumes and in the jovian magnetosphere were investigated by Graps (2001) and Flandes (2005). Dust measurements of the Cassini spacecraft at its Jupiter flyby in 2000 showed that the grains are mostly composed of sodium chloride (NaCl) formed by condensation in Io's volcanic plumes (Postberg et al., 2006). (ii) Dust clouds surrounding the Galilean moons which consist of mostly sub-micron grains (Krüger et al., 1999d, 2000, 2003c). These grains were ejected from the moons' surfaces by hypervelocity impacts of interplanetary dust particles (Krivov et al., 2003; Sremčević et al., 2003, 2005). (iii) Bigger micron-sized grains forming a tenuous dust ring between the Galilean moons. This group is composed of two sub-populations, one orbiting Jupiter on prograde orbits and a second one on retrograde orbits (Colwell et al., 1998b; Thiessenhusen et al., 2000). Most of the prograde population is maintained by grains escaping from the clouds that surround the Galilean moons (Krivov et al., 2002a,b). (iv) In November 2002 and September 2003 Galileo traversed Jupiter's gossamer ring and provided the first in situ measurements of a dusty planetary ring (Krüger, 2003; Moissl, 2005) which is also accessible with astronomical imaging techniques.

This is the eighth paper in a series dedicated to presenting both raw and reduced data from the Galileo and Ulysses dust instruments. Grün et al. (1995c, hereafter Paper I) described the reduction process of Galileo and Ulysses dust data. In Papers II, IV and VI (Grün et al., 1995a; Krüger et al., 1999a, 2001a) we present the Galileo data set spanning the seven year time period from October 1989 to December 1996. Papers III, V and VII (Grün et al., 1995b; Krüger et al., 1999c, 2001b) provide nine years of Ulysses data from October 1990 to December 1999. The present paper extends the Galileo data set from January 1997 to December 1999, which covers the second half of Galileo's prime Jupiter mission and the entire Galileo Europa mission. A companion paper (Krüger et al., 2006, Paper IX) presents Ulysses' measurements from 2000 to 2004.

The main data products are a table of the number of all impacts determined from the particle accumulators and a table of both raw and reduced data of all "big" impacts received on the ground. The information presented in these papers is similar to data which we are submitting to the various data archiving centres (Planetary Data System, NSSDC, etc.). The only difference is that the paper version does not contain the full data set of the large number of "small" particles, and the numbers of impacts deduced from the accumulators are typically averaged over several days. Electronic access to the complete data set including the numbers of impacts deduced from the accumulators in full time resolution is also possible via the world wide web: http://www.mpi-hd.mpg.de/dustgroup/.

This paper is organised similarly to our previous papers. Section 2 gives a brief overview of the Galileo mission until the end of 1999, the dust instrument and lists important mission events in the time interval 1997–1999 considered in this paper. A description of the new Galileo dust data set for 1997–1999 together with a discussion of the detected noise and dust impact rates is given in Section 3. Section 4 analyses and discusses various characteristics of the new data set. Finally, in Section 5 we discuss results on jovian dust achieved with the new data set.

2. Mission and instrument operations

2.1. Galileo mission

Galileo was launched on 18 October 1989. Two flybys at Earth and one at Venus between 1990 and 1992 gave the spacecraft enough energy to leave the inner solar system. During its interplanetary voyage Galileo had close encounters with the asteroids Gaspra and Ida, and on 7 December 1995 the spacecraft arrived at Jupiter and was injected into a highly elliptical orbit about the planet, becoming the first spacecraft orbiting a planet of the outer solar system. Galileo performed 34 revolutions about Jupiter until September 2003 when the mission was terminated with the spacecraft impacting the planet.

Galileo's trajectory during its orbital tour about Jupiter from January 1997 to December 1999 is shown in Fig. 1. Galileo had regular close flybys at Jupiter's Galilean moons. 19 such encounters occurred in the 1997–1999 interval (six at Callisto, two at Ganymede, nine at Europa

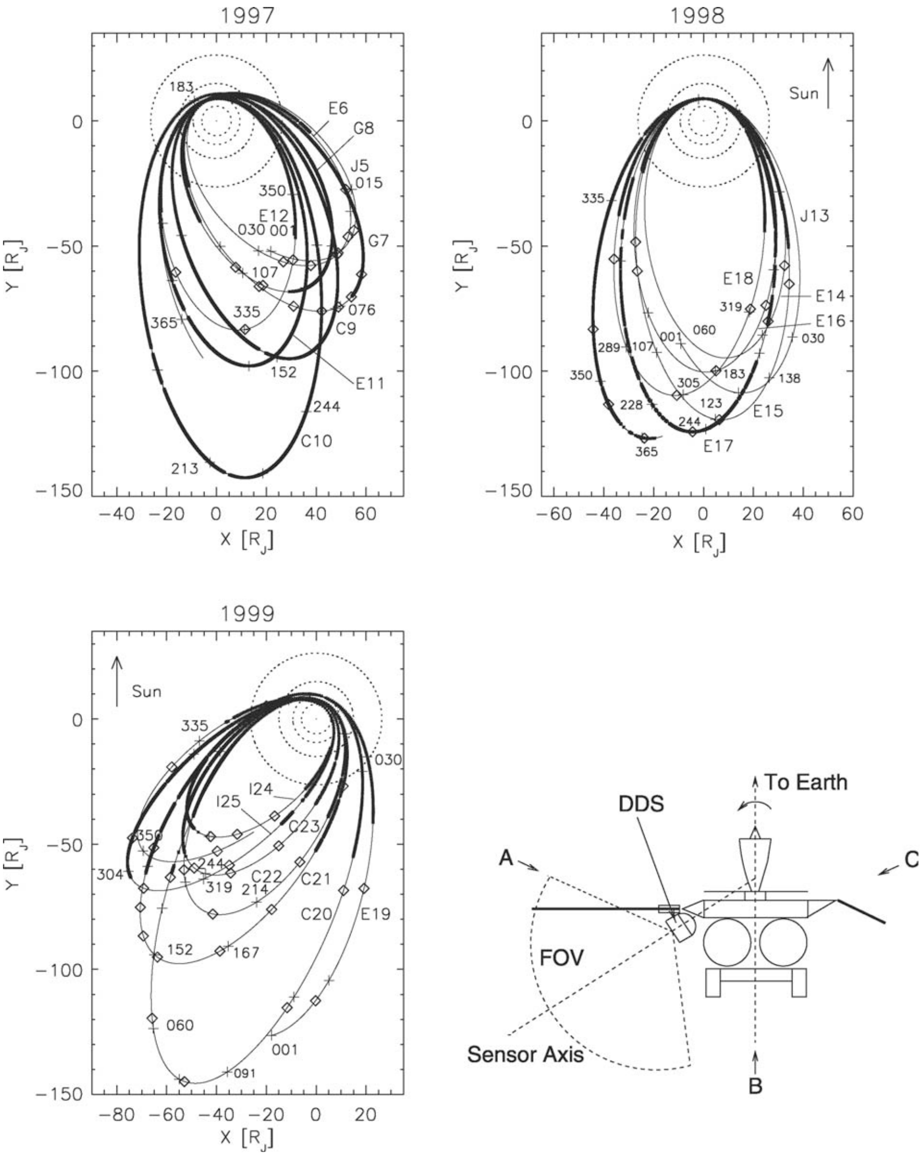

Fig. 1. Galileo's trajectory in the jovian system from 1997 to 1999 in a Jupiter-centric coordinate system (thin solid line). Crosses mark the spacecraft position at about 15 day intervals (days of year are indicated). Periods when RTS data were obtained are shown as thick solid lines, MROs are marked by diamonds. Galileo's orbits are labelled 'E6', 'G7', 'G8', 'C9', 'C10', 'E11'–'E19', 'C20'–'C23', 'I24', 'I25'. Sun direction is to the top and the Sun and Earth directions coincide to within 10°. The orbits of the Galilean moons are indicated (dotted lines). The sketch of the Galileo spacecraft shows the dust detector (DDS), its geometry of dust detection and its field-of-view (FOV). The spacecraft antenna usually pointed towards Earth and the spacecraft made about 3 revolutions per minute. Arrows indicate the approach directions of the dust stream particles at the times of onset (A), 180° shift (B) and cessation (C) of the streams (see text and Fig. 11 for details).

and two at Io, cf. Table 1). Galileo orbits are labelled with the first letter of the Galilean moon which was the encounter target during that orbit, followed by the orbit number. For example, "E6" refers to Galileo's sixth orbit about Jupiter which had a close flyby at Europa. Satellite flybys occurred within two days of Jupiter closest approach (pericentre passage). Detailed descriptions of the Galileo mission and the spacecraft were given by Johnson et al. (1992) and D'Amario et al. (1992).

Galileo was a dual spinning spacecraft with an antenna that pointed antiparallel to the positive spin axis. During most of the initial 3 years of the mission the antenna pointed towards the Sun (cf. Paper II). Since 1993 the antenna was usually pointed towards Earth. Deviations from the Earth pointing direction in 1997–1999, the time period considered in this paper, are shown in Fig. 2. Sharp spikes in the pointing deviation occurred when the spacecraft was turned away from the nominal Earth direction for dedicated imaging observations with Galileo's cameras or for orbit trim maneuvers with the spacecraft thrusters. These spikes lasted typically several hours. Table 1 lists significant mission and dust instrument events for 1997–1999. Comprehensive lists of earlier events can be found in Papers II, IV and VI.

Table 1
Galileo mission and dust detector (DDS) configuration, tests and other events (1997–1999)

Yr-day	Date	Time	Event
89-291	18 Oct 1989	16:52	Galileo launch
95-341	07 Dec 1995	21:54	Galileo Jupiter closest approach, distance: $4.0R_J$
96-355	20 Dec 1996	06:43	DDS configuration: $HV = 2, EVD = C, I, SSEN = 0, 0, 1, 1, 18R_J$ from Jupiter
97-004	04 Jan 1997	14:30	Galileo OTM-18, duration 8 h, no attitude change
97-007	07 Jan 1997	21:12	DDS last MRO before solar conjunction
97-008	08 Jan 1997	14:53	Galileo turn: 6°, new nominal attitude
97-010	10 Jan 1997		Start solar conjunction period
97-019	19 Jan 1997	01:55	DDS configuration: $EVD = I, SSEN = 0, 1, 1, 1, 18R_J$ from Jupiter
97-020	20 Jan 1997	00:27	Galileo Jupiter closest approach, distance $9.1R_J$
97-021	21 Jan 1997	10:00	DDS configuration: $EVD = C, I, SSEN = 0, 0, 1, 1, 18R_J$ from Jupiter
97-028	28 Jan 1997		End solar conjunction period
97-029	29 Jan 1997	05:08	DDS first MRO after solar conjunction
97-037	06 Feb 1997	10:00	Galileo OTM-19, duration 9 h, no attitude change
97-041	10 Feb 1997	18:38	Galileo turn: 6°, new nominal attitude
97-048	17 Feb 1997	05:59	DDS begin RTS data
97-049	18 Feb 1997	17:00	Galileo OTM-20, duration 4.5 h, no attitude change
97-050	19 Feb 1997	17:35	DDS configuration: $EVD = I, SSEN = 0, 1, 1, 1, 18R_J$ from Jupiter
97-051	20 Feb 1997	16:37	DDS end RTS data, begin record data
97-051	20 Feb 1997	17:06	**Galileo Europa 6 (E6) closest approach**, altitude 586 km
97-051	20 Feb 1997	17:22	DDS end record data, begin RTS data
97-051	20 Feb 1997	20:54	Galileo Jupiter closest approach, distance $9.1R_J$
97-053	22 Feb 1997	00:10	DDS configuration: $EVD = C, I, SSEN = 0, 0, 1, 1, 18R_J$ from Jupiter
97-054	23 Feb 1997	01:25	DDS end RTS data
97-055	24 Feb 1997	04:00	Galileo OTM-21, duration 3 h, no attitude change
97-072	13 Mar 1997	22:15	Galileo OTM-22, size of turn 2°, duration 18 h, no attitude change
97-075	16 Mar1997	02:30	DDS begin RTS data
97-076	17 Mar 1997	07:30	Galileo turn: 9°, new nominal attitude
97-091	01 Apr 1997	04:40	Galileo OTM-23, duration 8 h, no attitude change
97-092	02 Apr 1997	00:03	DDS noise test, duration 4 h
97-092	02 Apr 1997	04:17	DDS configuration: $EVD = C, I, SSEN = 0, 0, 1, 1$
97-093	03 Apr 1997	07:55	DDS configuration: $EVD = I, SSEN = 0, 1, 1, 1, 18R_J$ from Jupiter
97-094	04 Apr 1997	05:59	Galileo Europa closest approach, altitude 24600 km
97-094	04 Apr 1997	11:04	Galileo Jupiter closest approach, distance $9.1R_J$
97-095	05 Apr 1997	06:44	DDS end RTS data, begin record data
97-095	05 Apr 1997	07:10	**Galileo Ganymede 7 (G7) closest approach**, altitude 3102 km
97-095	05 Apr 1997	07:40	DDS end record data, begin RTS data
97-095	05 Apr 1997	14:24	DDS configuration: $EVD = I, C, SSEN = 0, 0, 1, 1, 18R_J$ from Jupiter
97-098	08 Apr 1997	09:31	DDS end RTS data
97-098	08 Apr 1997	08:00	Galileo OTM-24, duration 9 h, no attitude change
97-108	18 Apr 1997	09:46	DDS begin RTS data
97-108	18 Apr 1997	18:00	Galileo turn 6°, new nominal attitude
97-111	21 Apr 1997	10:00	OTM-25, duration 5 h, no attitude change
97-124	04 May 1997	17:00	OTM-26, duration 5 h, no attitude change
97-125	05 May 1997	10:48	Galileo turn 10°, duration 66 h, return to nominal attitude
97-127	07 May 1997	09:00	DDS configuration: $EVD = I, SSEN = 0, 1, 1, 1, 18R_J$ from Jupiter
97-127	07 May 1997	15:36	DDS end RTS data, begin record data
97-127	07 May 1997	15:56	**Galileo Ganymede 8 (G8) closest approach**, altitude 1603 km
97-127	07 May 1997	16:22	DDS end record data, begin RTS data
97-128	08 May 1997	11:42	Galileo Jupiter closest approach, distance $9.2R_J$
97-129	09 May 1997	14:37	DDS configuration: $EVD = I, C, SSEN = 0, 0, 1, 1, 18R_J$ from Jupiter
97-131	11 May 1997	02:00	Galileo OTM-27, duration 8 h, no attitude change
97-154	03 Jun 1997	03:00	Galileo OTM-28, duration 5 h, no attitude change
97-174	23 Jun 1997	06:18	Galileo OTM-29, duration 5 h, no attitude change
97-176	25 Jun 1997	07:58	Galileo turn22°, duration 12 h, return to nominal attitude
97-176	25 Jun 1997	13:26	DDS end RTS data, begin record data
97-176	25 Jun 1997	13:48	**Galileo Callisto 9 (C9) closest approach**, altitude 418 km
97-176	25 Jun 1997	14:11	DDS end record data, begin RTS data
97-177	26 Jun 1997	10:00	DDS configuration: $EVD = I, SSEN = 0, 1, 1, 1, 18R_J$ from Jupiter
97-177	26 Jun 1997	17:20	Galileo Ganymede closest approach, altitude 79,740 km
97-178	27 Jun 1997	11:52	Galileo Jupiter closest approach, distance $10.8R_J$
97-179	28 Jun 1997	14:09	DDS configuration: $EVD = C, I, SSEN = 0, 0, 1, 1, 18R_J$ from Jupiter
97-191	10 Jul 1997	18:00	Galileo OTM-30, duration 10 h, no attitude change
97-195	14 Jul 1997	02:38	Galileo turn 6°, duration 11 h, return to nominal attitude

Table 1 (*continued*)

Yr-day	Date	Time	Event
97-220	08 Aug 1997	00:00	DDS noise test, duration 4 h
97-220	08 Aug 1997	17:45	Galileo OTM-31, duration 7 h, no attitude change
97-221	09 Aug 1997	16:38	Galileo turn 7°, new nominal attitude
97-235	23 Aug 1997	00:00	DDS configuration: HV = 3
97-247	04 Sep 1997	20:05	Galileo turn 64°, duration 5 h, return to nominal attitude
97-253	10 Sep 1997	10:03	Galileo turn 51°, duration 5 h, return to nominal attitude
97-256	13 Sep 1997	00:00	DDS configuration: HV = 2
97-257	14 Sep 1997	02:00	Galileo OTM-32, duration 5 h, no attitude change
97-259	16 Sep 1997	23:47	DDS end RTS data, begin record data
97-260	17 Sep 1997	00:19	**Galileo Callisto 10 (C10) closest approach**, altitude 538 km
97-260	17 Sep 1997	00:50	DDS end record data, begin RTS data
97-260	17 Sep 1997	20:32	DDS configuration: EVD = I, SSEN = 0, 1, 1, 1, 18 R_J from Jupiter
97-261	18 Sep 1997	23:10	Galileo Jupiter closest approach, altitude 9.2 R_J
97-262	19 Sep 1997	08:23	Galileo turn 27°, duration 33 h, return to nominal attitude
97-263	20 Sep 1997	02:12	DDS configuration: EVD = C, I, SSEN = 0, 0, 1, 1, 18 R_J from Jupiter
97-263	20 Sep 1997	21:30	Galileo OTM-33, duration9 h, no attitude change
97-278	05 Oct 1997	20:00	Galileo turn 86°, duration 12 h, return to nominal attitude
97-286	13 Oct 1997	12:00	DDS noise test, duration 4 h
97-291	18 Oct 1997	16:00	Galileo OTM-34, duration 14 h, no attitude change
97-302	29 Oct 1997	19:00	Galileo OTM-35, no attitude change
97-309	05 Nov 1997	21:26	DDS configuration: EVD = I, SSEN = 0, 1, 1, 1, new nominal configuration, 18 R_J from Jupiter
97-310	06 Nov 1997	20:09	DDS end RTS data, begin record data
97-310	06 Nov 1997	20:32	**Galileo Europa 11 (E11) closest approach**, altitude 2039 km
97-310	06 Nov 1997	21:01	DDS end record data, begin RTS data
97-311	07 Nov 1997	00:42	Galileo Jupiter closest approach, altitude 9.0 R_J
97-311	07 Nov 1997	10:40	Galileo turn 40°, duration 38 h, return to nominal attitude
97-313	09 Nov 1997	10:23	DDS noise test, duration 4 h
97-314	10 Nov 1997	00:57	Galileo OTM-36, no attitude change
97-315	11 Nov 1997	02:00	DDS end RTS data
97-325	21 Nov 1997	21:00	Galileo turn 4°, new nominal attitude
97-330	26 Nov 1997	19:26	Galileo OTM-37, no attitude change
97-343	09 Dec 1997	15:00	DDS begin RTS data
97-347	13 Dec 1997	23:36	Galileo OTM-38, no attitude change
97-350	16 Dec 1997	06:35	Galileo Jupiter closest approach, altitude 8.8 R_J
97-350	16 Dec 1997	11:42	DDS end RTS data, begin record data
97-350	16 Dec 1997	12:03	**Galileo Europa 12 (E12) closest approach**, altitude 201 km
97-350	16 Dec 1997	12:28	DDS end record data, begin RTS data
97-354	20 Dec 1997	06:00	DDS end RTS data before solar conjunction
97-355	21 Dec 1997	02:16	Galileo OTM-39, size of turn 18°, duration 47 h, 8° off Earth direction after turn
98-012	12 Jan 1998	09:36	Galileo turn 15°, new nominal attitude
98-016	16 Jan 1998	04:00	DDS configuration: HV = 1, EVD = I, SSEN = 0, 1, 1, 1
98-017	17 Jan 1998	07:00	Galileo turn 30°, duration 4 h, return to nominal attitude
98-023	23 Jan 1998	01:11	Galileo OTM-40, no attitude change
98-035	03 Feb 1998	02:00	Galileo turn 3°, new nominal attitude
98-039	08 Feb 1998	01:03	Galileo OTM-41, no attitude change
98-041	10 Feb 1998	17:58	**Galileo Europa 13A (E13A) closest approach**, altitude 3557 km
98-041	10 Feb 1998	23:09	Galileo Jupiter closest approach, distance 8.9 R_J
98-044	13 Feb 1998	12:16	Galileo OTM-42, no attitude change
98-045	14 Feb 1998		Start solar conjunction period
98-063	04 Mar 1998		End solar conjunction period
98-067	08 Mar 1998	09:15	Galileo turn 7°, new nominal attitude
98-069	10 Mar 1998	22:00	Galileo turn 60°, duration 4 h, return to nominal attitude
98-072	13 Mar 1998	21:41	Galileo OTM-43, no attitude change
98-079	20 Mar 1998	02:06	Galileo turn 4°, new nominal attitude
98-080	21 Mar 1998	20:00	DDS configuration: HV = 2, EVD = I, SSEN = 0, 1, 1, 1
98-080	21 Mar 1998	22:59	DDS first MRO after solar conjunction
98-083	24 Mar 1998	13:59	DDS begin RTS
98-085	26 Mar 1998	21:11	Galileo OTM-44, no attitude change
98-088	29 Mar 1998	07:59	Galileo Jupiter closest approach, distance 8.8 R_J
98-088	29 Mar 1998	13:05	DDS end RTS data, begin record data
98-088	29 Mar 1998	13:21	**Galileo Europa 14 (E14) closest approach**, altitude 1644 km
98-088	29 Mar 1998	14:00	DDS end record data, begin RTS data

Table 1 (*continued*)

Yr-day	Date	Time	Event
98-090	31 Mar 1998	19:28	DDS end RTS data
98-090	31 Mar 1998	23:00	Galileo OTM-45, size of turn 60°, duration 3 h, return to nominal attitude
98-100	10 Apr 1998	14:15	Galileo turn 4°, new nominal attitude
98-114	24 Apr 1998	02:00	Galileo turn 2°, new nominal attitude
98-125	05 May 1998	12:00	Galileo OTM-46, size of turn 50°, duration 3 h, return to nominal attitude
98-136	16 May 1998	00:00	Galileo turn 10°, duration 4 h, return to nominal attitude
98-145	25 May 1998	11:39	DDS begin RTS data
98-148	28 May 1998	17:10	DDS last RTS data before spacecraft anomaly
98-148	28 May 1998	19:15	Galileo OTM-47, no attitudechange
98-148	28 May 1998	20:21	Galileo spacecraft anomaly
98-149	29 May 1998	19:17	DDS begin RTS data after spacecraft anomaly
98-151	31 May 1998	20:42	DDS end RTS data, begin record data
98-151	31 May 1998	21:13	**Galileo Europa 15 (E15) closest approach**, altitude 2515 km
98-151	31 May 1998	21:43	DDS end record data, begin RTS data
98-152	01 Jun 1998	02:35	Galileo Jupiter closest approach, distance 8.8 R_J
98-154	03 Jun 1998	14:08	DDS end RTS data
98-156	05 Jun 1998	16:36	Galileo OTM-48, no attitude change
98-177	26 Jun 1998	16:36	Galileo OTM-49, no attitude change
98-182	01 Jul 1998	00:00	Galileo turn 7°, duration 4 h, return to nominal attitude
98-194	13 Jul 1998	23:39	DDS begin RTS data
98-196	15 Jul 1998	10:39	Galileo OTM-50, no attitude change
98-201	20 Jul 1998	17:23	DDS last RTS data before spacecraft anomaly
98-201	20 Jul 1998	17:38	Galileo spacecraft anomaly
98-202	20 Jul 1998	00:18	Galileo Jupiter closest approach, distance 8.9 R_J
98-202	21 Jul 1998	05:04	**Galileo Europa 16 (E16) closest approach**, altitude 1834 km
98-205	24 Jul 1998	00:12	DDS begin RTS data after spacecraft anomaly
98-212	31 Jul 1998	15:36	Galileo OTM-51, size of turn 2°, duration 2 h, return to nominal attitude
98-230	18 Aug 1998	01:00	Galileo turn 2°, new nominal attitude
98-236	24 Aug 1998	15:56	Galileo OTM-52, no attitude change
98-259	16 Sep 1998	01:00	Galileo turn 6°, new nominal attitude
98-265	22 Sep 1998	14:06	Galileo OTM-53, no attitude change
98-269	26 Sep 1998	03:54	**Galileo Europa 17 (E17) closest approach**, altitude 3582 km
98-269	26 Sep 1998	08:26	Galileo Jupiter closest approach, distance 8.9 R_J
98-274	01 Oct 1998	08:23	DDS end RTS data
98-296	23 Oct 1998	19:26	Galileo OTM-55, no attitude change
98-321	17 Nov 1998	07:30	DDS begin RTS data
98-323	19 Nov 1998	18:06	Galileo OTM-56, no attitude change
98-326	22 Nov 1998	04:04	DDS last RTS data before spacecraft anomaly
98-326	22 Nov 1998	05:41	Galileo spacecraft anomaly
98-326	22 Nov 1998	07:31	Galileo Jupiter closest approach, distance 8.9 R_J
98-326	22 Nov 1998	11:38	**Galileo Europa 18 (E18) closest approach**, altitude 2271 km
98-327	23 Nov 1998	03:31	DDS begin RTSdata after spacecraft anomaly
98-329	25 Nov 1998	16:36	Galileo OTM-57, no attitude change
98-352	18 Dec 1998	16:06	Galileo OTM-58, no attitude change
98-357	23 Dec 1998	14:24	Galileo turn 6°, new nominal attitude
98-364	30 Dec 1998	23:57	DDS end RTS data
99-022	22 Jan 1999	00:00	Galileo turn 3°, new nominal attitude
99-027	27 Jan 1999	19:00	DDS begin RTS data
99-028	28 Jan 1999	20:06	Galileo OTM-59, no attitude change
99-031	31 Jan 1999	18:00	Galileo turn 60°, duration 1.5 h, Galileo pointing 60° off Earth direction
99-032	01 Feb 1999	01:49	DDS end RTS data, begin record data
99-032	01 Feb 1999	02:20	**Galileo Europa 19 (E19) closest approach**, altitude 1439 km
99-032	01 Feb 1999	05:02	Galileo Jupiter closest approach, distance 9.1 R_J
99-032	01 Feb 1999	02:39	DDS end record data, last data before spacecraft anomaly
99-032	01 Feb 1999	04:45	Galileo turn 40°*
99-032	01 Feb 1999	05:41	Galileo spacecraft anomaly (Galileo pointing 40° off Earth)
99-037	06 Feb 1999		Galileo turn 6°
99-038	07 Feb 1999		Galileo turn 34°, return to nominal attitude (Earth pointing)
99-041	10 Feb 1999	02:08	DDS begin RTS data after spacecraft anomaly
99-042	11 Feb 1999	15:08	DDS end RTS data
99-048	17 Feb 1999	01:00	Galileo turn 4°, new nominal attitude
99-064	05 Mar 1999	07:00	Galileo turn 3°, new nominal attitude
99-074	15 Mar 1999	00:00	Galileo turn 13°, new nominal attitude
99-078	19 Mar 1999	12:36	Galileo OTM-61, no attitude change

Table 1 (*continued*)

Yr-day	Date	Time	Event
99-078	19 Mar 1999	07:58	DDS last MRO before solar conjunction
99-081	22 Mar 1999		Start solar conjunction period
99-100	10 Apr 1999		End solar conjunction period
99-105	15 Apr 1999	01:58	DDS first MRO after solar conjunction
99-107	17 Apr 1999	00:00	Galileo turn 8°, newnominal attitude
99-118	28 Apr 1999	00:00	DDS begin RTS data
99-123	03 May 1999	17:00	Galileo Jupiter closest approach, distance 9.4R_J
99-125	05 May 1999	13:56	**Galileo Callisto 20 (C20) closest approach**, altitude 1321 km
99-125	05 May 1999	14:38	DDS end RTS data, begin record data
99-125	05 May 1999	15:17	DDS end record data, begin RTS data
99-129	09 May 1999	02:23	Galileo OTM-63, no attitude change
99-137	17 May 1999	16:39	DDS end RTS data
99-142	22 May 1999	04:00	Galileo turn 7°, new nominal attitude
99-155	04 Jun 1999	20:16	Galileo OTM-64, no attitude change
99-167	16 Jun 1999	04:00	Galileo turn 3°, new nominal attitude
99-175	24 Jun 1999	14:00	Galileo turn 3°, duration 10 h, return to nominal attitude
99-176	25 Jun 1999	19:06	Galileo OTM-65, no attitude change
99-177	26 Jun 1999	22:00	DDS begin RTS data
99-181	30 Jun 1999	07:47	**Galileo Callisto 21 (C21) closest approach**, altitude 1048 km
99-181	30 Jun 1999	08:10	DDS end RTS data, begin record data
99-181	30 Jun 1999	08:31	DDS end record data, begin RTS data
99-183	02 Jul 1999	05:05	Galileo Jupiter closest approach, distance 7.3R_J
99-185	04 Jul 1999	02:00	Galileo turn 4°, duration 2 h, return to nominal attitude
99-189	08 Jul 1999	12:00	Galileo OTM-66, no attitude change
99-190	09 Jul 1999	17:08	DDS end RTS data
99-190	09 Jul 1999	18:00	Galileo turn 3°, new nominal attitude
99-204	23 Jul 1999	18:36	Galileo OTM-67, no attitude change
99-210	29 Jul 1999	00:00	Galileo turn 7°, duration 3 h, return to nominal attitude
99-220	08 Aug 1999	23:17	DDS begin RTS data
99-223	11 Aug 1999	08:31	Galileo OTM-68, no attitude change
99-224	12 Aug 1999	10:59	Galileo Jupiter closest approach, distance 7.3R_J
99-226	14 Aug 1999	08:31	**Galileo Callisto 22 (C22) closest approach**, altitude 2299 km
99-228	16 Aug 1999	00:00	Galileo OTM-69, size of turn 3°, duration 2 h, return to nominal attitude
99-238	26 Aug 1999	11:29	DDS end RTS data
99-242	30 Aug 1999	16:06	Galileo OTM-70, size of turn 7°, duration 3 h, return to nominal attitude
99-255	12 Sep 1999	00:41	DDS begin RTS data
99-257	14 Sep 1999	19:58	Galileo Jupiter closest approach, distance 6.5R_J
99-259	16 Sep 1999	17:27	**Galileo Callisto 23 (C23) closest approach**, altitude 1052 km
99-260	17 Sep 1999	12:00	Galileo turn 2°, duration 2 h, return to nominal attitude
99-264	21 Sep 1999	00:00	Galileo OTM-72, size of turn 2°, duration 2 h, return to nominal attitude
99-271	28 Sep 1999	01:00	Galileo OTM-73, size of turn 2°, duration 2 h, return to nominal attitude
99-272	29 Sep 1999	00:45	DDS end RTS data
99-274	01 Oct 1999	21:00	Galileo turn 4°, new nominal attitude
99-281	08 Oct 1999	22:33	DDS begin RTS data
99-283	10 Oct 1999	09:00	DDS last RTS data before spacecraft anomaly
99-283	10 Oct 1999	09:17	Galileo spacecraft anomaly
99-283	10 Oct 1999	21:46	DDS begin RTS data after spacecraft anomaly
99-284	11 Oct 1999	02:03	Galileo Jupiter closest approach, distance 5.5R_J
99-284	11 Oct 1999	03:41	DDS end RTS data
99-284	11 Oct 1999	04:33	**Galileo Io 24 (I24) closest approach**, altitude 611 km
99-284	11 Oct 1999	04:48	DDS begin RTS data
99-287	14 Oct 1999	01:00	Galileo turn 5°, return to nominal attitude
99-288	15 Oct 1999	16:36	Galileo OTM-75, no attitude change
99-299	26 Oct 1999	20:00	Galileo turn 6°, new nominal attitude
99-305	01 Nov 1999	08:04	DDS end RTS data
99-305	01 Nov 1999	18:44	DDS configuration: HV = 3
99-306	02 Nov 1999	12:36	Galileo OTM-76, no attitude change
99-314	10 Nov 1999	19:36	Galileo OTM-76A, no attitude change
99-326	22 Nov 1999	04:00	DDS begin RTS data
99-330	26 Nov 1999	02:09	Galileo Jupiter closest approach, distance 5.7R_J
99-330	26 Nov 1999	04:05	**Galileo Io 25 (I25) closest approach**, altitude 300 km
99-332	28 Nov 1999	23:32	DDS end RTS data
99-334	30 Nov 1999	01:00	Galileo OTM-77, size of turn 3°, duration 6 h, return to nominal attitude
99-343	09 Dec1999	08:00	Galileo turn 7° duration 3 h, return to nominal attitude

Table 1 (*continued*)

Yr-day	Date	Time	Event
99-345	11 Dec 1999	02:07	DDS configuration: HV = 4
99-348	14 Dec 1999	13:01	Galileo OTM-79, no attitude change
99-355	21 Dec 1999	20:26	Galileo OTM-80, no attitude change
99-357	23 Dec 1999	08:00	Galileo turn 3°, new nominal attitude
99-365	31 Dec 1999	08:36	Galileo OTM-81, no attitude change

See text for details. Abbreviations used: MRO: DDS memory readout; HV: channeltron high voltage step; EVD: event definition, ion-(I), channeltron-(C), or electron-channel (E); SSEN: detection thresholds, ICP, CCP, ECP and PCP; OTM: orbit trim maneuver; RTS: Realtime science.

*Galileo pointing cannot be restored between 099-032, 04:45 h and 99-037 because of spacecraft anomaly.

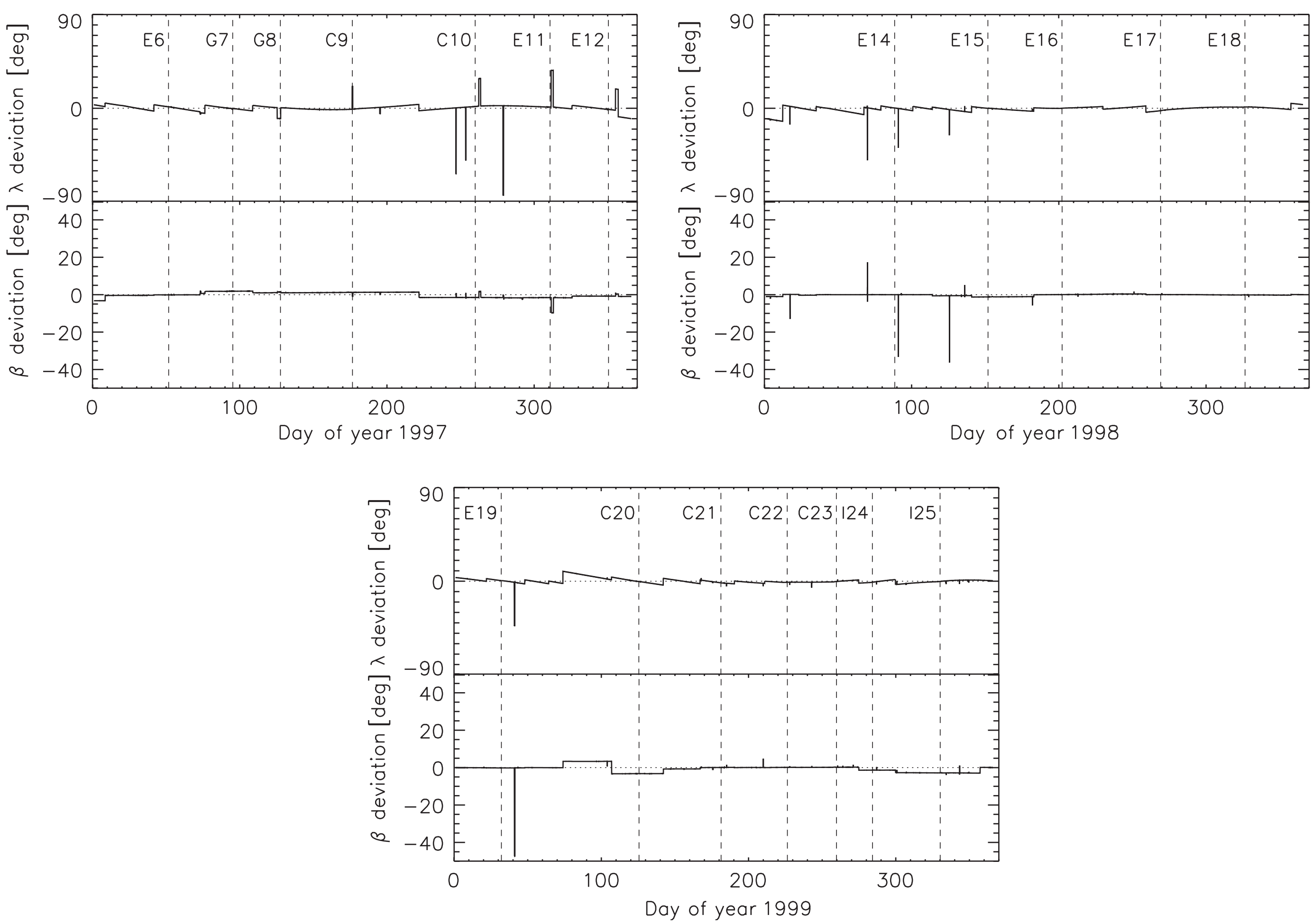

Fig. 2. Spacecraft attitude: deviation of the antenna pointing direction (i.e. negative spin axis) from the Earth direction. The angles are given in ecliptic longitude (λ) and latitude (β, equinox 1950.0). The targeted encounters of Galileo with the Galilean moons are indicated by dotted lines. Sharp spikes are associated with imaging observations with Galileo's cameras or orbit trim maneuvers with the spacecraft thrusters.

2.2. *Dust detection geometry*

The Dust Detector System (DDS) was mounted on the spinning section of Galileo and the sensor axis was offset by 60° from the positive spin axis (an angle of 55° was erroneously stated in earlier publications). A schematic view of the Galileo spacecraft and the geometry of dust detection is shown in Fig. 1.

The rotation angle measured the viewing direction of the dust sensor at the time of a dust impact. During one spin revolution of the spacecraft the rotation angle scanned through a complete circle of 360°. At rotation angles of 90° and 270° the sensor axis lay nearly in the ecliptic plane, and at 0° it was close to the ecliptic north direction. DDS rotation angles are taken positive around the negative spin axis of the spacecraft. This is done to easily compare

Galileo spin angle data with those taken by Ulysses, which, unlike Galileo, has its positive spin axis pointed towards Earth.

The nominal field-of-view of the DDS sensor target is 140°. A smaller field-of-view applies to a subset of jovian dust stream particle impacts—the so-called class 3 impacts in amplitude range AR1 (Krüger et al., 1999b, cf. Paper I and Section 3 for a definition of these parameters) while the nominal target size should be applied to class 2 jovian dust stream impacts. For all impacts which are not due to jovian dust stream particles a larger field-of-view of 180° should be applied because the inner sensor side wall turned out to be almost as sensitive to dust impacts as the target itself (Altobelli et al., 2004; Willis et al., 2004, 2005).

During one spin revolution of the spacecraft the sensor axis scanned a cone with 120° opening angle towards the anti-Earth direction. Dust particles that arrived from within 10° of the positive spin axis (anti-Earth direction) could be detected at all rotation angles, whereas those that arrived at angles from 10° to 130° from the positive spin axis could be detected over only a limited range of rotation angles. Note that these angles refer to the nominal sensor field-of-view of 140°.

2.3. *Data transmission*

In June 1990 DDS was reprogrammed for the first time after launch and since then the DDS memory could store 46 instrument data frames (with each frame comprising the complete data set of an impact or noise event, consisting of 128 bits, plus ancillary and engineering data; cf. Papers I and II). DDS time-tagged each impact event with an 8 bit word allowing for the identification of 256 unique steps. In 1990 the step size of this time word was set to 4.3 h. Hence, the total accumulation time after which the time word was reset and the time labels of older impact events became ambiguous was $256 \times 4.3\,\mathrm{h} = 46$ days.

During a large fraction of Galileo's orbital mission about Jupiter dust detector data were transmitted to Earth in the so-called realtime science mode (RTS). In RTS mode, DDS data were read out either every 7.1 or every 21.2 min, depending on the spacecraft data transmission rate, and directly transmitted to Earth with a rate of 3.4 or 1.1 bits per second, respectively. For short periods (i.e. $\sim \pm \frac{1}{2}$ h) around closest approaches to the Galilean moons (cf. Table 1), DDS data were collected with a higher rate of about 24 bits per second, recorded on the tape recorder (record mode) and transmitted to Earth up to several weeks later. Sometimes RTS data for short time intervals were also stored on the tape recorder and transmitted later but this did not change the labelling—they are also called RTS.

In RTS and record mode the time between two readouts of the instrument memory determined the number of events in a given time period for which their complete information could be transmitted. Thus, the complete information on each impact was transmitted to Earth when the impact rate was below one impact per either 7.1 or 21.2 min in RTS mode or one impact per minute in record mode, respectively. If the impact rate exceeded these values, the detailed information of older events was lost because the full data set of only the latest event was stored in the DDS memory.

Furthermore, in RTS and record mode the time between two readouts also determined the accuracy with which the impact time is known. Hence, the uncertainty in the impact time is 7.1 or 21.2 min in RTS mode and about one minute in record mode, respectively. During times when only MROs occurred, the accuracy was limited by the increment of the DDS internal clock, i.e. 4.3 h.

In RTS and record mode only seven instrument data frames were read out at a time and transmitted to Earth rather than the complete instrument memory. Six of the frames contained the information of the six most recent events in each amplitude range. The seventh frame belonged to an older event read out from the instrument memory (FN = 7) and was transmitted in addition to the six new events. The position in the instrument memory from which this seventh frame was read changed for each readout so that after 40 readouts the complete instrument memory was transmitted (note that the contents of the memory may have changed significantly during the time period of 40 readouts if high event rates occurred).

RTS data were usually obtained when Galileo was in the inner jovian system where relatively high dust impact rates occurred. During time intervals when Galileo was in the outer jovian magnetosphere DDS data were frequently received as instrument memory-readouts (MROs). MROs returned event data which had accumulated in the instrument memory over time. The contents of all 46 instrument data frames of DDS was transmitted to Earth during an MRO. If too many events occurred between two MROs, the data sets of the oldest events became overwritten in the memory and were lost. Although the entire memory was read out during an MRO, the number of data sets of new events that could be transmitted to Earth in a given time period was much smaller than with RTS data because MROs occurred much less frequently (note that with MROs occurring at 20 day intervals the corresponding data transmission rate was only about 3×10^{-3} bits s^{-1}).

In 1997–1999, RTS and record data were obtained during a period of 449 days (Fig. 1) which amounts to 41% of the total 3-year period. During the remaining times when DDS was operated in neither RTS nor record mode, MROs occurred at approximately 2–3 week intervals. MROs were frequent enough so that no ambiguities in the time-tagging occurred (i.e. MROs occurred at intervals smaller than 46 days). The only exception is orbit 13 when no RTS data were obtained and the interval between two MROs was longer: RTS data ended before solar conjunction on day 97-354 and the next MRO occurred on day 98-080 so that one reset of the DDS internal clock happened in this period. Hence, it is not known if 14 dust impacts with impact date 98-041 and 98-042 have to be shifted to an impact date 46 days earlier. However, this is very unlikely because the impact times assigned to these particles are close to Galileo's perijove passage when usually the highest dust impact rates were recognised during other Galileo orbits (in particular in the higher amplitude ranges). Impact times shifted to 46 days earlier imply that these impacts would have happened around day 97-360 far away from Jupiter where only low impact rates were expected (cf. Fig. 3).

2.4. Dust instrument operation

During most of Galileo's interplanetary cruise the dust instrument was operated in the following configuration: the channeltron voltage was set to 1020 V (HV = 2), the event definition status was set such that the channeltron or the ion-collector channel could independently initiate a measurement cycle (EVD = C, I) and the detection thresholds for the charges on the ion-collector, channeltron, electron-channel and entrance grid were set (SSEN = 0, 0, 1, 1). During Galileo's first passage through the inner jovian system (G1 orbit, June 1996) after insertion into an orbit about Jupiter, strong channeltron noise was recorded with this configuration within about $20R_J$ distance from Jupiter (Jupiter radius, $R_J = 71,492$ km) which reached up to 10,000 events per minute (Paper VI). It caused significant dead time of the instrument. To prevent dead time due to channeltron noise, the event definition status was set such that only the ion channel could initiate a measurement cycle and the detection threshold for the channeltron charge was raised by one step while Galileo was within $18R_J$ from Jupiter during all later orbits of Galileo's prime Jupiter mission (i.e. until day 97-309) (cf. Table 1). This reduced the noise sensitivity in the inner jovian system and effectively prevented dead-time problems. During all orbits after the prime Jupiter mission (i.e. after day 97-309) this configuration was the nominal operational mode to simplify instrument operation. In this configuration, increased channeltron noise still occurred during short time intervals in the inner jovian system. However, the

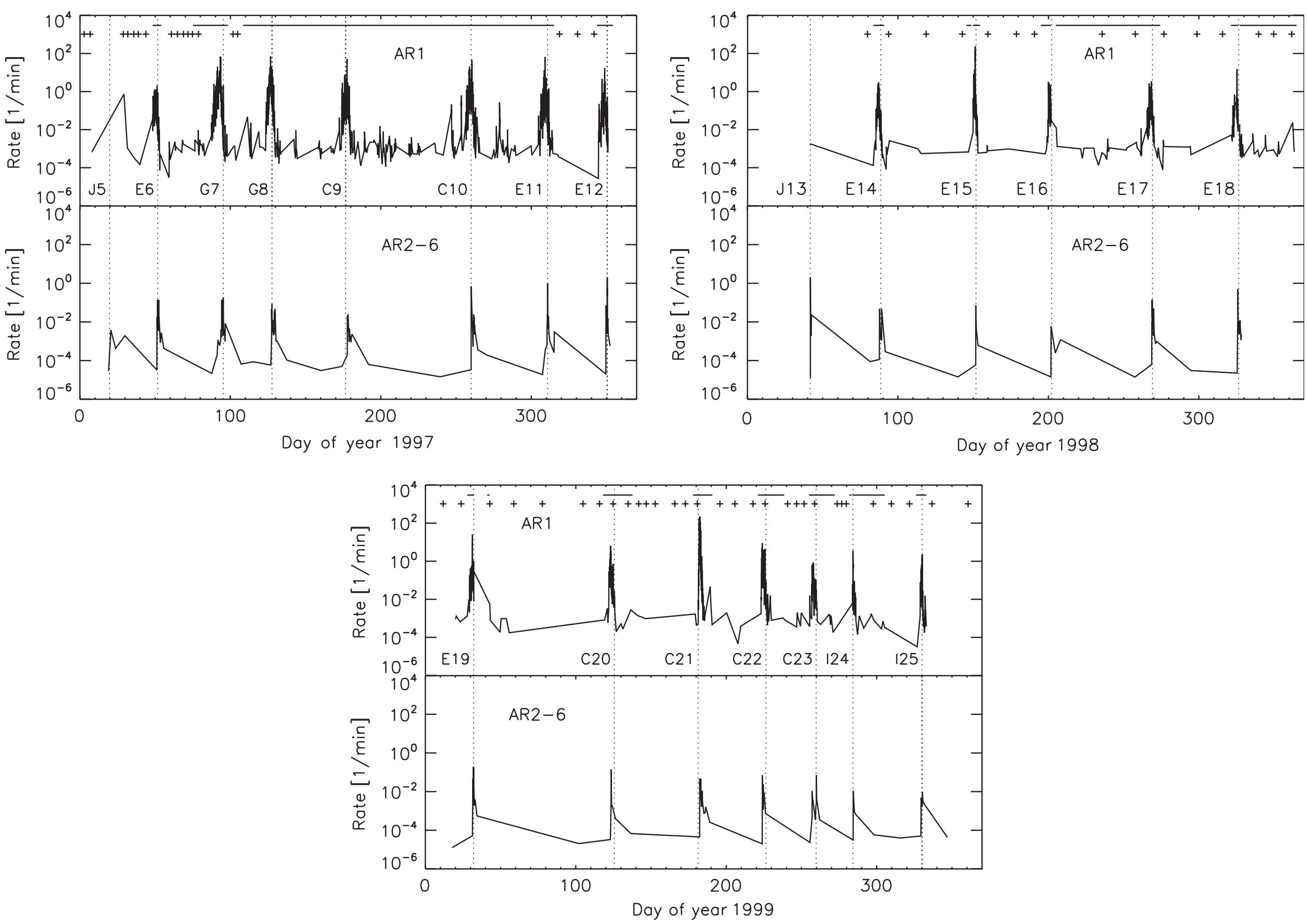

Fig. 3. Dust impact rate detected by DDS in 1997–1999. For each year the top panel shows the impact rate in AR1 which is dominated by the dust streams, the bottom panel that for the higher amplitude ranges AR2-6. Dotted lines indicate the closest approaches to the Galilean moons. Perijove passages occurred within two days of the moon closest approaches. These curves are plotted from the number of impacts with the highest time resolution which is available only in electronic form. No smoothing was applied to the data. In the top panels (AR1), time intervals with continuous RTS coverage are indicated by horizontal bars, memory readouts (MROs) are marked by crosses.

channeltron amplification had dropped due to degradation and this noise was sufficiently low that no dead time occurred anymore.

No reprogramming of the DDS onboard computer was necessary in the 1997–1999 time interval. In fact, the last reprogramming for the entire Galileo mission was performed on 4 December 1996 when two overflow counters were added (Paper VI). With these overflow counters no unrecognised accumulator overflows occurred in the 1997–1999 interval.

During the Jupiter orbital tour of Galileo, orbit trim maneuvers (OTMs) were executed around perijove and apojove passages to target the spacecraft to close encounters with the Galilean moons. Many of these maneuvers required changes in the spacecraft attitude off the nominal Earth pointing direction (cf. Fig. 2). Additionally, dedicated spacecraft turns occurred typically in the inner jovian system within a few days around perijove passage to allow for imaging observations with Galileo's cameras or to maintain the nominal Earth pointing direction. Specifically large turns happened on 4 September 1997 (97-247), 10 September 1997 (97-253), and 7 November 1997 (97-311). During these turns the spacecraft spin axis was oriented 64°, 51° and 40° away from the Earth direction, respectively. All three attitude changes were large enough that DDS could record impacts of dust stream particles at times when these grains would have been undetectable with the nominal spacecraft orientation (Figs. 3 and 4).

In the time interval considered in this paper a total of five spacecraft anomalies (safings) happened on days 98-148, 98-201, 98-326, 99-032, and 99-283. These anomalies always occurred in the inner jovian system in the region where the highest radiation levels were collected by the spacecraft and recovery usually took several days. Although DDS continued to measure dust impacts, the collected data could not be transmitted to Earth during the recovery and most of them were lost.

2.5. DDS electronics degradation

Analysis of the impact charges and rise times measured by DDS revealed strong degradation of the instrument electronics which was most likely caused by the harsh radiation environment in the inner jovian magnetosphere. A detailed analysis was published by Krüger et al. (2005). Here we recall the most significant results: (a) the sensitivity of the instrument for dust impacts and noise had dropped; (b) the amplification of the charge amplifiers had degraded, leading to reduced impact charge values Q_I and Q_E; (c) drifts in the target and ion collector rise time signals lead to prolonged rise times t_I and t_E; (d) degradation of the channeltron required increases in the channeltron voltage (on 99-305 and 99-345 in the time period considered in this paper). In particular, (a) requires a time-dependent correction when comparing dust fluxes early in the Galileo Jupiter mission with later measurements. (b) and (c) affect the mass and speed calibration of DDS. After 2000, masses and speeds derived from the instrument calibration have to be taken with caution because the electronics degradation was very severe. Only in cases where impact speeds are known from other arguments can corrected masses of particles be derived (e.g. the dust cloud measurements in the vicinity of the Galilean moons or Galileo's gossamer ring passages). On the other hand, given the uncertainty of a factor of two in the speed and that of a factor of ten in the mass, the increased uncertainty due to the electronics degradation is relatively small until the end of 1999 (it should be noted that the dust data until end 1996 published earlier (Papers II, IV and VI) remain unchanged). In particular, no corrections for dust fluxes, grain speeds and masses are necessary until end 1999 and results obtained with this data set in earlier publications remain valid. Beginning in 2000 the degradation has to be taken into account. For this reason, we will present 2000 and later data in a forthcoming paper.

3. Impact events

3.1. Event classification and noise

DDS classified all events—real dust impacts and noise events—into one of 24 different categories (six amplitude ranges for the charge measured on the ion collector grid and four event classes) and counted them in 24 corresponding 8 bit accumulators (Paper I). In interplanetary space most of the 24 categories were relatively free from noise and only sensitive to real dust impacts. The details of the noise behaviour in interplanetary space can be found in Papers II and IV.

In the extreme radiation environment of the jovian system, a different noise response of the instrument was recognised: especially within about $20 R_J$ from Jupiter classes 1 and 2 were contaminated with noise (Krüger et al., 1999b). However, this noise was different from the channeltron noise recorded in the G1 orbit (Paper VI). Analysis of the dust data set from Galileo's entire Jupiter mission showed that noise events could reliably be eliminated from class 2 (Krüger et al., 2005) while class 1 events show signatures of being nearly all noise in the jovian environment. We therefore consider the class 3 and the noise-removed class 2 impacts as the complete set of dust data from Galileo's Jupiter mission. Apart from a missing third charge signal—class 3 has three charge signals and class 2 only two—there is no physical difference between dust impacts categorised into class 2 or class 3. In particular, we usually classify all class 1 and class 0 events detected in the jovian environment as noise.

In this paper the terms "small" and "big" have the same meaning as in Papers IV and VI (which is different from the terminology of Paper II). Here, we call all particles in classes 2 and 3 in the amplitude ranges 2 and higher (AR2-6) "big". Particles in the lowest amplitude range (AR1) are called "small". This distinction separates the

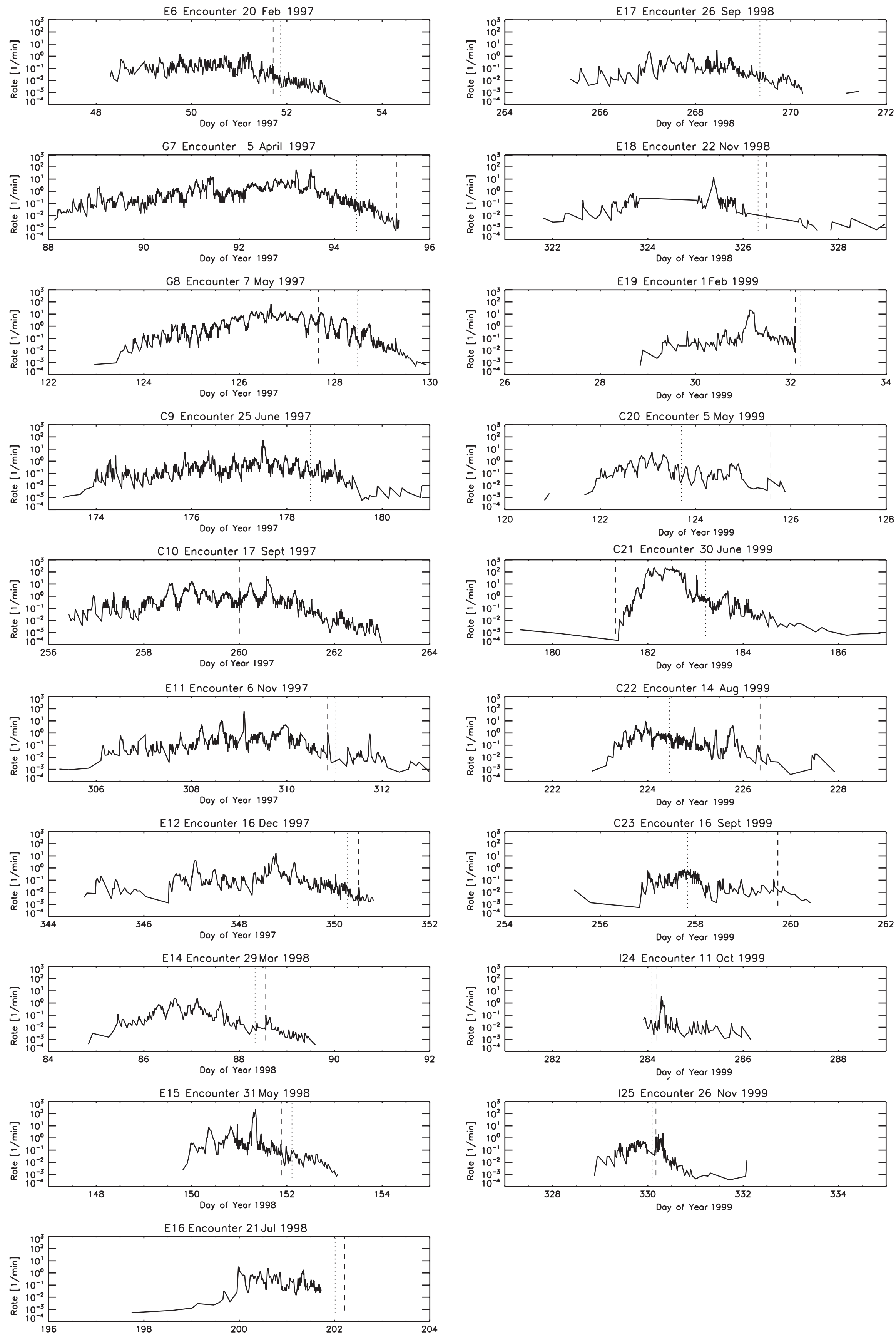

Fig. 4. Dust impact rate detected by DDS in the inner jovian system in higher time resolution. Only data for AR1 (classes 2 and 3) are shown. Dashed lines indicate perijove passage of Galileo, dotted lines closest approaches to the Galilean moons.

small jovian dust stream particles from bigger grains which are mostly detected between the Galilean moons (see also Section 5.2).

Table 2 lists the number of all dust impacts and noise events identified with DDS in the 1997–1999 interval as deduced from the accumulators of classes 2 and 3. Depending on the event rate the numbers are given in intervals from half a day to a few weeks (the numbers with the highest time resolution are available in electronic form only and are provided to the data archiving centres). For

Table 2
Overview of dust impacts accumulated with Galileo DDS between 1 January 1997 and 31 December 1999

Date	Time	D_{Jup} [R_J]	Δt [d]	$f_{noi,AC21}$	AC 21	AC 31	$f_{noi,AC22}$	AC 22	AC 32	$f_{noi,AC23}$	AC 23	AC 33	$f_{noi,AC24}$	AC 24	AC 34	$f_{noi,AC25}$	AC 25	AC 35	$f_{noi,AC26}$	AC 26	AC 36
97-006	11:56	70.93	7.667	–	–	–	1.00	1	–	–	–	–	–	–	–	–	–	–	–	–	–
97-043	12:38	60.43	37.02	0.12	22199	3289	0.23	22	1	0.00	2	–	0.00	3	1	–	–	–	–	–	–
97-050	00:07	24.77	6.478	0.26	904	120	–	–	–	–	–	–	–	–	–	–	–	–	–	–	–
97-052	06:49	11.00	2.279	0.34	825	58	0.33	12	1	–	–	3	–	–	1	0.00	1	–	–	–	–
97-087	19:12	57.45	35.51	0.84	158	2	0.50	2	2	0.00	3	2	–	–	1	0.00	1	–	–	–	–
97-092	08:40	27.22	4.561	0.15	6984	1078	0.00	2	–	–	–	–	–	–	–	–	–	–	–	–	–
97-097	05:12	32.32	4.855	0.18	13907	1677	0.19	16	5	0.00	3	3	0.00	1	1	–	–	–	–	–	–
97-124	09:09	41.87	27.16	0.54	180	–	1.00	4	1	–	–	–	–	–	–	–	–	–	–	–	–
97-126	05:37	28.45	1.853	0.14	4350	607	–	–	–	–	–	–	–	–	–	–	–	–	–	–	–
97-128	14:11	9.410	2.357	0.16	21305	2591	0.60	5	6	0.00	1	2	–	–	–	–	–	–	–	–	–
97-130	18:55	29.33	2.197	0.56	430	30	0.56	9	2	0.00	1	–	0.00	1	–	–	–	1	0.00	1	–
97-174	00:17	46.31	43.22	0.82	138	–	0.50	4	–	–	–	–	0.00	1	–	–	–	–	–	–	–
97-176	00:53	31.03	2.025	0.14	687	68	–	–	–	–	–	1	–	–	–	–	–	–	–	–	–
97-178	00:02	12.83	1.964	0.18	4546	372	–	–	1	–	–	–	0.00	1	1	–	–	–	–	–	–
97-180	03:21	23.55	2.138	0.52	1037	44	0.40	5	1	–	–	1	–	–	1	–	–	–	–	–	–
97-235	15:23	129.8	55.50	0.79	170	–	0.67	9	1	–	–	–	–	–	–	0.00	1	–	–	–	–
97-256	17:09	52.54	21.07	0.62	160	21	1.00	2	–	–	–	1	–	–	–	–	–	–	–	–	–
97-258	11:19	39.60	1.757	0.18	697	34	1.00	–	–	–	–	–	–	–	–	–	–	–	–	–	–
97-260	00:25	26.15	1.545	0.10	5842	812	–	–	2	–	–	–	–	–	–	–	–	–	–	–	–
97-262	09:34	11.23	2.380	0.27	6343	553	0.50	12	–	0.00	3	2	0.00	1	–	–	–	1	–	–	–
97-305	04:26	54.42	42.78	0.75	236	7	0.82	11	–	0.00	1	1	1.00	1	–	–	–	–	–	–	–
97-308	00:08	35.37	2.821	0.26	411	32	–	–	1	–	–	–	–	–	–	–	–	–	–	–	–
97-310	00:49	16.56	2.028	0.14	5000	472	0.00	1	–	–	–	–	–	–	–	–	–	–	–	–	–
97-313	07:11	28.60	3.265	0.56	513	34	0.75	10	2	0.00	7	3	0.00	1	1	–	–	1	–	–	–
97-345	01:55	49.01	31.78	0.82	96	2	0.86	7	–	–	–	–	–	–	–	–	–	–	–	–	–
97-348	00:49	28.27	2.953	0.14	789	57	1.00	1	–	–	–	–	–	–	–	–	–	–	–	–	–
97-350	23:47	13.57	2.957	0.21	2285	103	0.64	11	4	0.00	1	1	0.00	3	2	–	–	2	–	–	–
98-042	12:37	12.20	56.53	1.00	4704	137	0.77	22	4	0.00	1	3	–	–	1	0.00	1	–	–	–	–
98-085	13:45	33.29	43.04	0.20	19	4	0.00	4	1	–	–	–	–	–	–	–	–	–	–	–	–
98-088	02:16	9.580	2.521	0.19	1330	71	1.00	5	–	0.00	3	–	–	–	1	–	–	–	–	–	–
98-092	03:18	42.43	4.043	0.88	129	1	0.82	11	–	1.00	1	1	–	–	1	–	–	–	–	–	–
98-149	19:38	29.82	57.68	0.56	70	–	0.67	3	–	–	–	–	–	–	–	–	–	–	–	–	–
98-151	00:28	17.78	1.201	0.06	2127	107	–	–	–	–	–	–	–	–	–	–	–	–	–	–	–
98-153	05:34	18.08	2.212	0.24	16224	868	0.73	11	2	0.00	3	–	–	–	2	–	–	–	–	–	–
98-198	14:21	38.73	45.36	0.94	72	–	1.00	1	–	–	–	–	–	–	–	–	–	–	–	–	–
98-201	02:30	15.81	2.506	0.13	971	55	–	–	–	–	–	–	–	–	–	–	–	–	–	–	–
98-204	17:29	33.73	3.624	0.45	323	17	1.00	6	1	–	–	1	–	–	1	–	–	–	–	–	–
98-264	20:50	47.70	60.13	0.68	234	3	0.71	8	–	–	–	–	–	–	–	–	–	–	–	–	–
98-267	00:14	30.43	2.141	0.12	161	9	–	–	–	–	–	–	–	–	–	–	–	–	–	–	–
98-270	00:20	13.31	3.003	0.24	1163	61	0.47	19	7	0.00	2	2	0.00	2	2	–	–	–	–	–	–
98-322	00:08	45.75	51.99	0.65	109	1	0.80	5	–	0.00	1	1	0.00	1	–	–	–	–	–	–	–
98-325	16:30	12.97	3.681	0.20	2247	119	1.00	2	1	–	–	–	–	–	–	–	–	–	–	–	–
98-328	23:24	33.37	3.287	0.42	117	5	0.11	9	2	0.00	2	4	–	–	1	–	–	–	–	–	–
98-363	10:05	128.8	34.44	0.83	66	2	–	–	–	–	–	–	–	–	–	–	–	–	–	–	–
99-029	04:37	36.63	30.77	0.10	45	–	1.00	3	–	0.00	1	–	–	–	–	–	–	–	–	–	–
99-031	13:14	13.58	2.359	0.20	4280	191	0.60	5	1	–	–	–	–	–	–	–	–	–	–	–	–
99-032	08:36	9.410	0.806	0.38	114	1	0.00	2	5	–	–	3	–	–	2	–	–	1	0.00	1	–
99-120	19:56	35.69	88.47	0.49	172	3	0.00	2	1	–	–	1	0.00	1	1	–	–	–	–	–	–
99-123	05:59	11.71	2.418	0.16	1436	73	0.50	2	–	–	–	–	–	–	–	–	–	–	–	–	–
99-130	00:37	59.44	6.776	0.31	1162	26	0.38	8	1	–	–	–	–	–	–	–	–	–	–	–	–

Table 2 (*continued*)

Date	Time	D_{Jup} [R_J]	Δt [d]	$f_{noi,AC21}$	AC 21	AC 31	$f_{noi,AC22}$	AC 22	AC 32	$f_{noi,AC23}$	AC 23	AC 33	$f_{noi,AC24}$	AC 24	AC 34	$f_{noi,AC25}$	AC 25	AC 35	$f_{noi,AC26}$	AC 26	AC 36
99-180	03:26	36.84	50.11	0.73	47	–	0.67	3	–	–	–	–	–	–	–	–	–	–	–	–	–
99-182	08:07	15.37	2.194	0.49	87250	2011	1.00	2	–	–	–	–	–	–	–	–	–	–	–	–	–
99-184	14:58	21.36	2.285	0.50	134087	1616	0.74	57	2	–	–	–	0.50	2	–	–	–	–	0.00	1	–
99-223	07:12	18.59	38.67	0.76	60	1	0.67	3	1	0.00	1	1	–	–	–	–	–	–	–	–	–
99-225	10:24	16.53	2.133	0.49	3786	101	0.70	23	3	–	–	–	–	–	–	–	–	–	–	–	–
99-229	07:00	47.79	3.858	0.52	898	15	0.50	2	–	–	–	–	–	–	–	–	–	–	–	–	–
99-255	19:05	27.56	26.50	0.68	42	–	0.50	2	–	–	–	–	–	–	–	–	–	–	–	–	–
99-258	10:34	12.09	2.644	0.62	886	7	0.75	12	–	–	–	–	–	–	–	–	–	–	–	–	–
99-261	07:49	38.73	2.885	0.55	89	1	0.63	8	1	–	–	1	–	–	–	–	–	–	–	–	–
99-283	11:21	12.10	22.14	0.93	42	–	0.67	3	–	–	–	–	–	–	–	–	–	–	–	–	–
99-289	02:45	52.04	5.641	0.88	1256	9	0.88	24	–	0.00	1	–	–	–	–	–	–	–	–	–	–
99-329	03:29	16.75	40.03	0.67	35	2	0.80	5	–	–	–	1	–	–	–	–	–	–	–	–	–
99-331	00:13	16.36	1.864	0.68	1042	9	0.50	6	3	–	–	1	–	–	1	–	–	–	–	–	–
99-346	22:13	86.09	15.91	0.83	10	–	–	–	–	–	–	–	0.00	1	–	–	–	–	–	–	–
Events (counted)				–	366997	17589	–	424	66	–	38	40	–	20	22	–	4	6	–	3	–
Impacts (complete data)				–	4287	3051	–	106	66	–	27	40	–	13	22	–	4	6	–	3	–
All events (complete data)				0.46	7981	3051	0.70	340	66	0.16	31	40	0.13	15	22	0.00	4	6	0.00	3	–

The Jovicentric distance D_{Jup}, the lengths of the time interval Δt (days) from the previous table entry, and the corresponding numbers of impacts are given for the class 2 and 3 accumulators. The accumulators are arranged with increasing signal amplitude ranges (AR), e.g. AC31 means counter for CLN = 3 and AR = 1. The determination of the noise contamination f_{noi} in class 2 is described in Paper VI. The Δt in the first line (day 97-006) is the time interval counted from the last entry in Table 2 in Paper VI. The totals of counted impacts, of impacts with complete data, and of all events (noise plus impact events) for the entire period are given in Paper VI. For AR1-4 the complete data set was transmitted for only a fraction of all particles detected. f_{noi} has been estimated from the data sets transmitted.

impacts in these two classes in the lowest amplitude range AR1 the complete data set for only 3% of all detected events was transmitted, the remaining 97% of events were only counted. Nearly all data sets for events in higher amplitude ranges were transmitted, although a few were also lost in AR2-4. We give only the number of events in classes 2 and 3 because they have been shown to contain real dust impacts: class 3 is almost always noise free (although Krüger et al. (1999b) found indications for a very small number of noise events in class 3, AR1, in the inner jovian system). Class 2 is strongly contaminated by noise events in the inner jovian system (within about $15 R_J$ from Jupiter).

The data set we present here was noise-removed with exactly the criteria derived by Krüger et al. (1999b, 2005). Degradation of the DDS electronics was taken into account beginning in 1997. In particular, the data set of 1996 published in Paper VI is not affected by electronics degradation and remains unchanged. The derivation of the noise contamination factor f_{noi} for class 2 was described in the same publication and is not repeated here.

The noise identification criteria of Krüger et al. (1999b, 2005) applied to the Galileo dust data set were developed to separate the tiny Jupiter stream particles from noise events. However, they did not work very well to distinguish secondary ejecta grains detected during close flybys at the Galilean moons from noise events (Krüger et al., 2003c). We therefore had to apply a different technique to identify ejecta grains which was also described in Paper VI. In particular, no noise-removal was applied to the Ganymede and Callisto data because these moons are outside the region where strong noise was recognised in class 2. On the other hand, data from all Europa flybys were noise-removed according to the criteria given in Paper VI (their Table 4). Details of the analysis of the ejecta dust clouds were also described by Krüger et al. (2000, 2003c).

In the 1997–1999 interval Galileo had nine targeted flybys at Europa, six at Callisto, two at Ganymede and two at Io (Table 1). The spacecraft orientation with the antenna pointing towards Earth and the geometry of the flybys at the moons allowed for the detection of ejecta particles within the Hill spheres of these moons until early 1999 only (orbit E19). At all later orbits cloud particles could not be detected in the vicinity of the Galilean moons anymore because of unfavourable detection geometry. Cloud particles at Europa could be measured during only seven flybys because spacecraft anomalies prevented the detection of dust at Europa during flybys E16 and E18.

During all Europa flybys in 1997–1999 and at the G7 Ganymede flyby the detection geometry was such that ejecta grains could only be detected from rotation angles $180^\circ \leqslant \mathrm{ROT} \leqslant 360^\circ$ so that the impact direction (ROT) could be used as a good parameter to identify ejecta grains because stream particles and ejecta grains approached from opposite directions. During the two Callisto flybys with favourable detection geometry (C9 and C10) and the G8 Ganymede flyby, however, the stream particles approached from the same direction as the ejecta grains and the measured impact velocities of the dust particles had to be used as an additional parameter to identify ejecta grains

(Krüger et al., 2003c). The encounter velocity of Galileo was $8.2\,km\,s^{-1}$ during both Callisto flybys and $8.6\,km\,s^{-1}$ at the G8 Ganymede encounter, respectively. For these three flybys we therefore included only particles with a measured impact velocity below $10\,km\,s^{-1}$ in the data set to minimise contamination by noise events. On the other hand, for the Europa flybys and the G7 Ganymede flybys we did not restrict the velocity. For all moon flybys we included only particles within the approximate Hill radius of the moon, except for Europa where we used a larger altitude limit because this dust cloud may be more extended.

3.2. Dust impact rates

Fig. 3 shows the dust impact rate recorded by DDS in 1997–1999 as deduced from the classes 2 and 3 accumulators. The impact rate measured in the lowest amplitude range (AR1) and the one measured in the higher amplitude ranges (AR2-6) are shown separately because they reflect two distinct populations of dust. AR1 contains mostly stream particles which were measured throughout the jovian system. Bigger particles (AR2-6) were mostly detected in the region between the Galilean moons. This is illustrated in the diagram: the impact rate for AR1 gradually increased when Galileo approached the inner jovian system, whereas the rate for the bigger AR2-6 impacts showed narrow peaks close to Galileo's perijove passages. Note that the impact rate in AR1 was usually one to two orders of magnitude higher than that for the big particles. Diagrams showing the AR1 impact rate with a much higher time resolution are given in Fig. 4.

In the inner jovian system the impact rates of AR1 particles frequently exceeded $10\,min^{-1}$. More than 100 impacts per minute were recorded during the C21 Callisto flyby on day 99-182. This represents one of the highest dust ejection rates of Io recorded during the Galileo Jupiter mission (Krüger et al., 2003a). Such high rates could only be recorded in RTS mode after the 1996 reprogramming of DDS when two overflow counters were added to the classes 2 and 3 counters in AR1. With these overflow counters no unrecognised counter resets occurred in the 1997–1999 interval in these two categories.

3.3. Event tables

Table 3 lists the data sets for all 287 big particles detected in classes 2 and 3 between 1 January 1997 and 31 December 1999 for which the complete information exists. Class 2 particles were separated from noise by applying the criteria developed by Krüger et al. (1999b, 2005) except for the flybys at the Galilean moons (see above). We do not list the small stream particles (AR1) in Table 3 because their masses and velocities are outside the calibrated range of DDS and they are by far too numerous to be listed here. The complete information of a total of 7338 small dust particles was transmitted in 1997–1999. The stream particles are believed to be about 10 nm in size and their velocities exceed $200\,km\,s^{-1}$ (Zook et al., 1996). Any masses and velocities derived for these particles with existing calibration algorithms would be unreliable. The full data set for all 7625 particles is submitted to the data archiving centres and is available in electronic form. A total number of 16,803 events (dust plus noise in all amplitude ranges and classes) were transmitted in 1997–1999, each with a complete data set.

In Table 3 dust particles are identified by their sequence number and their impact time. Gaps in the sequence number are due to the omission of the small particles. The time error value (TEV) which was introduced for the data set from the Jupiter mission because of the large differences in the timing accuracy of DDS in the various data readout modes (see Paper VI for details) is listed next. Then the event category–class (CLN) and amplitude range (AR)—are given. Raw data as transmitted to Earth are displayed in the next columns: sector value (SEC) which is the spacecraft spin orientation at the time of impact, impact charge numbers (IA, EA, CA) and rise times (IT, ET), time difference and coincidence of electron and ion signals (EIT, EIC), coincidence of ion and channeltron signal (IIC), charge reading at the entrance grid (PA) and time (PET) between this signal and the impact. Then the instrument configuration is given: event definition (EVD), charge sensing thresholds (ICP, ECP, CCP, PCP) and channeltron high voltage step (HV). See Paper I for further explanation of the instrument parameters, except TEV which is introduced in Paper VI.

The next four columns in Table 3 give information about Galileo's orbit: ecliptic longitude and latitude (LON, LAT) and distance from Jupiter (D_{Jup}, in R_J). The next column gives the rotation angle (ROT) as described in Section 2. Whenever this value is unknown, ROT is arbitrarily set to 999. This occurs 19 times in the full data set that includes the small particles. Then follows the pointing direction of DDS at the time of particle impact in ecliptic longitude and latitude (S_{LON}, S_{LAT}). When ROT is not valid, S_{LON} and S_{LAT} are also useless and set to 999. Mean impact velocity (v) and velocity error factor (VEF, i.e. multiply or divide stated velocity by VEF to obtain upper or lower limits) as well as mean particle mass (m) and mass error factor (MEF) are given in the last columns. For VEF >6, both velocity and mass values should be discarded. This occurs for 780 impacts.

No intrinsic dust charge values are given (Svestka et al., 1996). Even though the charge carried by the dust grains is expected to be larger in the jovian magnetosphere than in interplanetary space the charge measured on the entrance grid of the dust instrument did not give any convincing results yet. Reliable charge measurements for interplanetary dust grains were recently reported for the Cassini dust detector (Kempf et al., 2004). These measurements may lead to an improved understanding of the charge measurements of Ulysses and Galileo in the future.

Entries for the parameter PA in Table 3 sometimes have values between 49 and 63 although the highest possible

Table 3
DPF data: No., impact time, TEV CLN, AR, SEC, IA, EA, CA, IT, ET, EIT, EIC, ICC, PA, PET, EVD, ICP, ECP, CCP, PCP, HV and evaluated data: LON, LAT, D_{Jup} (in R_J, Jupiter radius $R_J = 71492$km), rotation angle (ROT), instr. pointing (S_{LON}, S_{LAT}), speed (v, in kms^{-1}), speed error factor (VEF), mass (m, in grams) and mass error factor (MEF)

No.	IMP. DATE	TEV	CLN	AR	SEC	IA	EA	CA	IT	ET	EIT	EIC	ICC	PA	PET	EVD	ICP	ECP	CCP	PCP	HV	LON	LAT	D_{Jup}	ROT	S_{LON}	S_{LAT}	V	VEF	M	MEF
8234	97-019 01:55:11	259	3	2	137	11	15	5	11	13	9	0	1	3	31	5	0	1	1	1	2	298.9	−0.4	15.738	257	247	−10	7.4	1.6	3.3×10^{-12}	6.0
8240	97-020 08:07:06	259	3	4	125	28	27	13	6	10	5	0	1	47	0	5	0	1	1	1	2	298.9	−0.4	10.205	274	247	3	19.0	1.9	1.3×10^{-11}	10.5
8242	97-020 12:26:22	259	2	4	36	25	3	4	14	15	15	0	1	22	0	5	0	1	1	1	2	298.9	−0.4	11.590	39	343	39	2.0	1.9	3.2×10^{-10}	10.5
8245	97-023 18:05:34	259	2	3	214	19	15	6	11	0	13	0	1	13	5	1	0	1	0	1	2	299.2	−0.4	38.690	149	338	−44	2.3	1.9	4.7×10^{-10}	10.5
8253	97-038 03:12:40	259	2	2	100	10	13	0	8	0	12	0	0	2	31	1	0	1	0	1	2	300.7	−0.4	71.135	309	254	31	19.0	1.9	1.5×10^{-13}	10.5
8557	97-051 03:08:06	8	2	2	179	10	13	0	11	12	10	0	0	35	0	5	0	1	1	1	2	301.6	−0.5	14.059	198	283	−51	9.2	1.6	1.2×10^{-12}	6.0
8577	97-051 05:08:26	8	2	2	77	13	3	6	15	11	12	0	0	34	0	5	0	1	1	1	2	301.6	−0.5	13.254	342	284	51	2.0	1.9	6.5×10^{-11}	10.5
8589	97-051 08:05:23	8	3	3	148	20	23	15	8	10	8	0	1	43	0	5	0	1	1	1	2	301.6	−0.5	12.114	242	256	−22	10.7	1.6	9.9×10^{-12}	6.0
8591	97-051 10:19:51	8	2	2	66	11	5	8	10	15	0	1	1	3	31	5	0	1	1	1	2	301.6	−0.5	11.304	357	304	54	9.7	1.9	3.1×10^{-13}	10.5
8600	97-051 12:13:05	8	3	3	160	20	21	14	7	6	5	0	1	6	0	5	0	1	1	1	2	301.6	−0.5	10.677	225	262	−35	12.7	1.9	4.7×10^{-12}	10.5
8601	97-051 13:09:44	8	3	2	117	13	20	10	13	15	9	0	1	39	0	5	0	1	1	1	2	301.6	−0.5	10.389	285	254	12	2.3	1.9	3.7×10^{-10}	10.5
8603	97-051 13:59:15	8	2	2	204	10	21	4	11	3	13	0	0	21	0	5	0	1	1	1	2	301.6	−0.5	10.154	163	331	−51	7.2	1.9	5.8×10^{-12}	10.5
8604	97-051 13:59:15	8	3	4	123	25	31	22	5	5	5	0	1	47	0	5	0	1	1	1	2	301.6	−0.5	10.154	277	253	5	29.8	1.9	2.6×10^{-12}	10.5
8605	97-051 14:06:21	8	2	5	160	53	49	24	14	7	0	1	1	23	5	5	0	1	1	1	2	301.6	−0.5	10.121	225	262	−35	2.0	1.9	1.7×10^{-07}	10.5
8615	97-051 17:06:14	2	2	2	161	11	7	10	12	14	15	0	1	36	25	5	0	1	1	1	2	301.6	−0.5	9.433	224	263	−36	4.5	1.9	4.6×10^{-12}	10.5
8618	97-052 00:05:55	259	3	3	125	21	26	18	7	7	6	0	1	46	0	5	0	1	1	1	2	301.6	−0.5	9.338	274	253	3	19.9	1.6	2.9×10^{-12}	6.0
8619	97-052 00:27:09	8	2	2	131	12	19	15	13	11	0	1	1	47	12	5	0	1	1	1	2	301.6	−0.5	9.389	266	253	−3	2.3	1.9	2.6×10^{-10}	10.5
8620	97-052 04:49:03	8	2	2	158	14	4	9	14	15	15	0	1	39	0	5	0	1	1	1	2	301.6	−0.5	10.371	228	261	−33	2.0	1.9	8.8×10^{-11}	10.5
8623	97-052 09:03:50	8	3	2	132	12	20	14	11	12	14	0	1	38	0	5	0	1	1	1	2	301.6	−0.5	11.787	264	253	−4	7.2	1.9	6.7×10^{-12}	10.5
8624	97-052 09:10:55	8	2	3	117	21	26	20	12	13	10	0	1	45	0	5	0	1	1	1	2	301.6	−0.5	11.831	285	254	12	2.5	1.6	1.8×10^{-09}	6.0
8626	97-052 12:43:16	8	3	3	102	19	21	19	10	7	9	0	1	37	0	5	0	1	1	1	2	301.6	−0.5	13.207	307	259	29	11.9	2.3	5.1×10^{-12}	21.5
8627	97-052 13:32:47	8	3	4	23	24	28	9	5	3	5	0	1	47	0	5	0	1	1	1	2	301.6	−0.5	13.542	58	358	26	45.7	1.6	2.9×10^{-13}	6.0
8628	97-052 14:36:30	8	2	3	13	19	20	13	13	9	0	1	1	47	19	5	0	1	1	1	2	301.6	−0.5	13.979	72	1	15	2.0	1.9	1.3×10^{-09}	10.5
8630	97-053 10:55:13	259	2	3	220	22	26	22	11	10	0	1	1	45	0	5	0	1	1	1	2	301.7	−0.5	22.457	141	350	−39	5.2	1.9	1.9×10^{-10}	10.3
8631	97-053 21:09:39	8	3	3	18	20	22	7	7	5	8	0	1	43	0	1	0	1	0	1	2	301.7	−0.5	26.447	65	360	20	26.7	1.7	4.1×10^{-13}	7.3
8632	97-055 17:59:12	259	2	5	27	49	50	27	15	15	0	1	1	47	2	1	0	1	0	1	2	301.9	−0.5	41.208	52	356	30	11.8	11.8	3.8×10^{-10}	5858.3
8650	97-087 14:36:18	22	3	2	139	8	11	7	11	12	9	0	1	2	31	1	0	1	0	1	2	305.0	−0.5	58.382	255	261	−11	9.2	1.6	6.0×10^{-13}	6.0
9013	97-091 04:07:42	8	2	2	138	8	13	0	10	10	7	0	0	37	0	1	0	1	0	1	2	305.2	−0.5	36.934	256	261	−10	16.0	1.6	2.0×10^{-13}	6.0
9163	97-091 18:24:07	8	2	2	166	8	9	8	9	10	3	1	1	8	31	1	0	1	0	1	2	305.2	−0.5	32.286	217	275	−39	12.7	1.9	2.0×10^{-13}	10.5
9413	97-092 22:00:18	8	2	3	159	21	13	12	8	13	0	1	1	10	15	1	0	1	0	1	2	305.3	−0.6	22.040	226	270	−32	9.7	1.9	4.1×10^{-12}	10.5
9543	97-093 13:55:48	8	2	2	103	10	7	3	12	13	0	1	1	43	22	5	0	1	1	1	2	305.3	−0.6	15.392	305	265	29	4.5	1.9	4.0×10^{-12}	10.5
9585	97-093 18:03:31	8	3	3	139	21	23	20	6	10	9	0	1	41	0	5	0	1	1	1	2	305.3	−0.6	13.671	255	261	−11	15.0	1.6	5.0×10^{-12}	6.0

9663	97-094 04:12:12	8	3	3	162	22	24	15	6	10	10	0	1	40	0	5	0	1	1	1	2	305.3	−0.6	10.079	222	272	−35	15.0	1.6	7.4×10^{-12}	6.0
9665	97-094 04:40:31	8	2	2	176	11	11	5	14	15	0	1	1	47	30	5	0	1	1	1	2	305.3	−0.6	9.959	203	287	−47	2.0	1.9	1.7×10^{-10}	10.5
9666	97-094 04:47:37	8	2	2	162	13	20	3	15	15	9	0	0	11	28	5	0	1	1	1	2	305.3	−0.6	9.930	222	272	−35	2.0	1.9	6.7×10^{-10}	10.5
9678	97-094 06:47:56	8	3	2	114	9	11	11	11	12	7	0	1	3	31	5	0	1	1	1	2	305.3	−0.6	9.509	290	261	17	9.2	1.6	7.1×10^{-13}	6.0
9687	97-094 08:19:56	8	2	4	102	27	26	24	9	9	0	1	1	18	10	5	0	1	1	1	2	305.3	−0.6	9.284	307	265	30	7.2	1.9	1.5×10^{-10}	10.5
9689	97-094 08:34:06	8	2	2	82	12	15	9	14	14	0	1	1	4	31	5	0	1	1	1	2	305.3	−0.6	9.258	335	283	49	2.5	1.6	1.4×10^{-10}	6.0
9698	97-094 11:38:06	8	2	2	185	15	10	3	14	5	14	0	0	30	3	5	0	1	1	1	2	305.3	−0.6	9.131	190	302	−51	2.0	1.9	2.7×10^{-10}	10.5
9701	97-094 12:27:39	8	2	2	61	11	12	5	15	15	0	1	1	47	29	5	0	1	1	1	2	305.3	−0.6	9.166	4	321	56	2.0	1.9	2.0×10^{-10}	10.5
9704	97-094 13:38:27	8	2	2	94	11	20	4	15	14	12	0	0	8	0	5	0	1	1	1	2	305.3	−0.6	9.268	318	270	38	2.0	1.9	4.8×10^{-10}	10.5
9705	97-094 13:38:27	8	3	4	90	28	31	14	4	5	5	0	1	47	0	5	0	1	1	1	2	305.3	−0.6	9.268	323	274	42	39.6	1.9	1.4×10^{-12}	10.5
9723	97-094 20:55:34	50	2	2	131	15	21	1	0	12	0	1	1	18	31	5	0	1	1	1	2	305.3	−0.6	10.974	266	259	−2	3.2	2.0	1.7×10^{-10}	12.5
9724	97-094 21:04:20	8	2	2	78	14	20	2	15	14	12	0	0	11	0	5	0	1	1	1	2	305.3	−0.6	11.023	340	288	52	2.5	1.6	2.9×10^{-10}	6.0
9725	97-094 22:15:06	8	3	3	106	19	21	11	9	7	8	0	1	1	0	5	0	1	1	1	2	305.3	−0.6	11.428	301	263	26	15.0	1.7	2.9×10^{-12}	7.1
9726	97-095 06:49:31	61	2	2	106	12	15	0	11	12	9	0	0	36	0	5	0	1	1	1	2	305.3	−0.6	14.815	301	263	26	9.2	1.6	2.1×10^{-12}	6.0
9734	97-095 07:09:37	2	3	2	133	13	19	9	10	9	9	0	1	4	31	5	0	1	1	1	2	305.3	−0.6	14.958	263	259	−4	14.0	1.6	1.2×10^{-12}	6.0
9736	97-095 07:15:03	2	3	2	105	8	10	5	11	12	6	0	1	4	31	5	0	1	1	1	2	305.3	−0.6	14.997	302	263	27	9.2	1.6	5.1×10^{-13}	6.0
9737	97-095 08:08:39	8	3	2	186	9	11	6	13	14	10	0	1	3	24	5	0	1	1	1	2	305.3	−0.6	15.375	188	303	−52	2.7	1.6	3.5×10^{-11}	6.0
9739	97-095 15:27:27	8	2	3	141	21	20	6	5	3	0	1	1	5	10	1	0	1	0	1	2	305.3	−0.6	18.439	252	262	−13	29.8	1.9	2.3×10^{-13}	10.5
9740	97-095 19:13:57	8	2	2	35	9	18	10	15	1	0	1	1	6	5	1	0	1	0	1	2	305.3	−0.6	19.988	41	359	39	2.0	1.9	2.7×10^{-10}	10.5
9741	97-096 12:06:05	8	3	2	121	15	31	3	9	6	5	0	1	26	0	1	0	1	0	1	2	305.4	−0.6	26.477	280	260	9	12.7	1.9	1.4×10^{-11}	10.5
9749	97-107 03:48:51	259	3	2	106	10	15	5	11	11	8	0	1	36	0	1	0	1	0	1	2	306.5	−0.6	72.537	301	264	26	12.1	1.6	7.9×10^{-13}	6.0
10496	97-127 09:49:05	8	3	2	121	11	14	9	11	13	8	0	1	0	31	5	0	1	1	1	2	308.2	−0.6	17.568	280	255	9	7.4	1.6	2.9×10^{-12}	6.0
10499	97-127 10:10:19	8	3	2	128	8	11	8	11	12	8	0	1	3	31	5	0	1	1	1	2	308.2	−0.6	17.420	270	255	0	9.2	1.6	6.0×10^{-13}	6.0
10565	97-127 15:55:21	2	2	2	152	9	11	0	11	12	6	0	0	3	31	5	0	1	1	1	2	308.2	−0.6	14.982	236	260	−26	9.2	1.6	7.1×10^{-13}	6.0
10575	97-127 16:07:15	2	3	3	131	19	21	23	10	7	8	0	1	38	0	5	0	1	1	1	2	308.2	−0.6	14.896	266	255	−2	11.9	2.3	5.1×10^{-12}	21.5
10624	97-127 20:23:03	8	3	3	149	21	23	23	6	7	9	0	1	43	0	5	0	1	1	1	2	308.2	−0.6	13.134	240	259	−22	24.4	1.6	7.5×10^{-13}	6.0
10638	97-127 22:37:31	8	3	2	139	9	11	10	11	12	8	0	1	0	0	5	0	1	1	1	2	308.2	−0.6	12.259	255	256	−11	9.2	1.6	7.1×10^{-13}	6.0
10670	97-128 02:02:47	8	3	2	85	13	19	2	11	10	9	0	1	36	0	5	0	1	1	1	2	308.2	−0.6	11.045	330	285	46	9.2	1.6	3.3×10^{-12}	6.0
10678	97-128 03:20:39	8	3	2	143	11	14	6	10	12	7	0	1	2	31	5	0	1	1	1	2	308.2	−0.6	10.640	249	267	−16	10.7	1.6	1.1×10^{-12}	6.0
10701	97-128 05:20:58	8	3	2	107	10	4	8	11	14	12	0	1	2	22	5	0	1	1	1	2	308.2	−0.6	10.094	300	269	24	7.2	1.9	5.4×10^{-13}	10.5
10714	97-128 08:39:08	8	2	2	216	12	15	2	9	10	5	0	0	4	0	5	0	1	1	1	2	308.2	−0.6	9.471	146	358	−42	18.3	1.6	3.2×10^{-13}	6.0
10784	97-128 18:47:49	8	2	2	29	10	14	0	9	10	4	0	0	43	0	5	0	1	1	1	2	308.2	−0.6	10.289	49	8	33	18.3	1.6	2.0×10^{-13}	6.0
10793	97-128 23:45:06	8	2	2	147	14	20	0	15	15	10	0	0	11	30	5	0	1	1	1	2	308.2	−0.6	11.883	243	268	−20	2.5	1.6	2.9×10^{-10}	6.0
10797	97-129 05:46:03	8	2	3	175	19	22	13	14	6	0	1	1	47	13	5	0	1	1	1	2	308.2	−0.6	14.263	204	290	−47	8.6	5.2	1.3×10^{-11}	343.5
10798	97-129 06:28:31	8	2	6	185	56	11	27	7	0	4	1	1	28	1	5	0	1	1	1	2	308.2	−0.6	14.559	190	307	−52	12.7	1.9	3.3×10^{-11}	10.5
10801	97-129 11:25:47	8	2	4	11	25	22	12	4	8	0	1	1	58	31	5	0	1	1	1	2	308.2	−0.6	16.660	75	14	13	39.6	1.9	2.3×10^{-13}	10.5
10802	97-129 14:36:53	8	2	2	247	10	13	0	9	10	5	0	0	11	1	1	0	1	0	1	2	308.2	−0.6	18.020	103	14	−9	18.3	1.6	1.7×10^{-13}	6.0
10803	97-129 14:58:07	8	3	5	16	49	51	25	15	8	6	0	1	3	31	1	0	1	0	1	2	308.2	−0.6	18.171	68	13	19	26.5	2.0	2.6×10^{-11}	12.5

Table 3 (*continued*)

No.	IMP. DATE	TEV	CLN	AR	SEC	IA	EA	CA	IT	ET	EIT	EIC	IIC	PA	PET	EVD	ICP	ECP	CCP	PCP	HV	LON	LAT	D_{Jup}	ROT	S_{LON}	S_{LAT}	V	VEF	M	MEF
10804	97-129 15:40:35	8	3	2	27	13	19	12	13	13	13	0	1	47	2	1	0	1	0	1	2	308.2	−0.6	18.472	52	9	31	2.7	1.6	1.6×10^{-10}	6.0
10805	97-130 08:20:55	259	3	2	144	8	14	7	15	15	11	0	1	40	5	1	0	1	0	1	2	308.3	−0.6	25.312	248	267	−17	2.1	1.6	1.3×10^{-10}	6.0
10809	97-137 13:14:34	22	2	4	248	24	28	25	12	12	0	1	1	45	4	1	0	1	0	1	2	309.0	−0.6	70.256	101	15	−8	2.5	1.6	4.1×10^{-09}	6.0
10812	97-156 02:26:05	22	2	2	241	11	14	4	14	15	15	0	1	5	8	1	0	1	0	1	2	310.8	−0.7	99.506	111	13	−16	2.1	1.6	2.0×10^{-10}	6.0
10816	97-160 04:48:58	22	2	2	219	8	14	0	0	0	12	0	0	3	31	1	0	1	0	1	2	311.2	−0.7	95.376	142	1	−39	11.8	11.8	5.4×10^{-13}	5858.3
10834	97-174 03:35:40	8	3	3	3	20	23	6	8	5	5	0	1	43	0	1	0	1	0	1	2	312.4	−0.7	45.387	86	15	4	23.3	2.0	7.8×10^{-13}	13.5
11375	97-177 17:05:03	8	2	4	115	24	22	19	13	13	0	1	1	11	19	5	0	1	1	1	2	312.6	−0.7	15.249	288	266	15	2.0	1.9	4.1×10^{-09}	10.5
11382	97-177 17:54:35	8	3	4	132	24	27	14	7	10	10	0	1	42	0	5	0	1	1	1	2	312.6	−0.7	14.938	264	265	−3	12.2	1.6	2.8×10^{-11}	6.0
11416	97-177 22:30:36	8	3	2	134	9	13	10	13	14	8	0	1	3	31	5	0	1	1	1	2	312.6	−0.7	13.308	262	265	−6	2.7	1.6	4.8×10^{-11}	6.0
11455	97-178 03:56:12	8	2	2	86	12	4	3	15	14	12	0	0	20	0	5	0	1	1	1	2	312.6	−0.7	11.754	329	284	45	2.0	1.9	6.3×10^{-11}	10.5
11461	97-178 04:38:40	8	3	3	147	21	23	20	7	7	9	0	1	43	0	5	0	1	1	1	2	312.6	−0.7	11.594	243	268	−20	19.9	1.6	1.7×10^{-12}	6.0
11548	97-178 23:02:48	8	3	2	112	13	14	5	11	11	9	0	1	39	0	5	0	1	1	1	2	312.6	−0.7	12.621	293	267	19	7.2	1.9	4.6×10^{-12}	10.5
11572	97-179 10:22:16	8	3	4	140	25	29	17	6	5	6	0	1	47	0	5	0	1	1	1	2	312.6	−0.7	16.690	253	266	−13	32.6	1.6	1.5×10^{-12}	6.0
11574	97-180 04:53:28	8	3	2	124	14	21	10	11	7	8	0	1	41	0	1	0	1	0	1	2	312.6	−0.7	24.172	276	265	5	7.2	1.9	1.1×10^{-11}	10.5
11577	97-180 20:41:54	22	2	5	41	49	50	25	15	15	3	1	1	22	1	1	0	1	0	1	2	312.6	−0.7	30.290	32	358	44	11.8	11.8	3.8×10^{-10}	5858.3
11585	97-189 10:11:23	22	2	2	233	9	9	8	11	12	15	0	1	10	2	1	0	1	0	1	2	313.4	−0.7	84.028	122	10	−25	7.2	1.9	1.1×10^{-12}	10.5
11610	97-239 11:17:15	22	3	3	103	21	26	13	5	5	5	0	1	46	0	1	0	1	0	1	3	318.1	−0.8	122.044	305	266	26	40.9	1.6	2.0×10^{-13}	6.0
12222	97-260 00:21:51	2	3	2	159	12	14	8	11	13	9	0	1	0	0	1	0	1	0	1	2	319.8	−0.8	26.167	226	267	−35	7.4	1.6	3.5×10^{-12}	6.0
12224	97-260 00:23:16	2	3	2	121	11	13	13	12	12	8	0	1	36	0	1	0	1	0	1	2	319.8	−0.8	26.158	280	260	7	7.3	1.6	2.7×10^{-12}	6.0
12512	97-261 07:51:06	8	2	2	6	9	8	4	11	14	13	0	0	6	31	5	0	1	1	1	2	319.9	−0.8	13.091	82	9	5	7.2	1.9	8.9×10^{-13}	10.5
12516	97-261 09:23:06	8	2	2	144	10	11	5	14	14	0	1	1	4	31	5	0	1	1	1	2	319.9	−0.8	12.481	248	261	−19	2.0	1.9	1.4×10^{-10}	10.5
12518	97-261 11:58:50	8	3	3	107	22	25	19	6	10	9	0	1	45	0	5	0	1	1	1	2	319.9	−0.8	11.506	300	264	22	15.0	1.6	8.8×10^{-12}	6.0
12524	97-261 13:45:00	8	2	2	102	8	4	3	12	14	12	0	0	2	31	5	0	1	1	1	2	319.9	−0.8	10.899	307	266	28	4.5	1.9	1.7×10^{-12}	10.5
12530	97-261 16:41:56	8	2	3	165	20	14	4	7	15	0	1	1	60	30	5	0	1	1	1	2	319.9	−0.8	10.039	218	271	−41	12.7	1.9	2.3×10^{-12}	10.5
12531	97-261 17:17:19	8	2	2	67	14	15	9	11	13	0	1	1	3	23	5	0	1	1	1	2	319.9	−0.8	9.895	356	308	52	7.2	1.9	6.0×10^{-12}	10.5
12532	97-261 18:06:52	8	2	3	85	20	12	6	10	12	15	1	1	39	20	5	0	1	1	1	2	319.9	−0.8	9.713	330	280	43	4.5	1.9	3.2×10^{-11}	10.5
12535	97-261 20:14:16	8	2	2	197	12	20	3	15	14	12	0	0	12	0	5	0	1	1	1	2	319.9	−0.8	9.358	173	325	−56	2.0	1.9	5.7×10^{-10}	10.5
12537	97-261 22:42:55	8	2	3	169	22	21	17	11	15	0	1	1	49	31	5	0	1	1	1	2	319.9	−0.8	9.175	212	275	−45	2.3	1.9	1.4×10^{-09}	10.5
12540	97-262 07:12:31	8	3	3	62	20	27	8	12	15	12	0	1	26	0	5	0	1	1	1	2	319.9	−0.8	10.473	3	318	52	2.0	1.9	4.9×10^{-09}	10.5
12542	97-262 08:37:27	8	2	2	147	10	12	3	12	13	3	1	1	4	31	5	0	1	1	1	2	319.9	−0.8	10.914	243	261	−22	5.9	1.6	3.8×10^{-12}	6.0
12543	97-262 09:34:04	8	3	5	128	52	50	24	9	8	5	0	1	47	0	5	0	1	1	1	2	319.9	−0.8	11.232	270	259	0	7.2	1.9	2.5×10^{-09}	10.5
12546	97-262 12:52:14	8	2	4	200	25	28	10	15	13	0	1	1	22	31	5	0	1	1	1	2	319.9	−0.8	12.453	169	331	−55	2.5	1.6	4.8×10^{-09}	6.0
12550	97-264 11:27:58	22	2	2	168	10	15	1	14	0	9	0	1	23	0	1	0	1	0	1	2	320.0	−0.8	31.180	214	274	−44	2.0	1.9	2.6×10^{-10}	10.5
12552	97-266 23:51:46	22	2	3	19	23	15	25	14	0	6	0	1	47	0	1	0	1	0	1	2	320.2	−0.8	49.528	63	5	20	2.0	1.9	1.6×10^{-09}	10.5
12553	97-270 14:55:10	22	3	3	71	23	29	3	6	4	5	0	1	47	0	1	0	1	0	1	2	320.6	−0.9	68.348	350	301	51	36.5	1.6	7.4×10^{-13}	6.0

12652	97-307 11:10:10	8	3	2	129	9	12	2	10	11	7	0	1	2	31	1	0	1	0	1	2	324.1	−0.9	39.545	269	259	−2	14.0	1.6	3.0×10^{-13}	6.0
13090	97-310 10:03:54	8	2	3	103	20	15	17	10	0	10	0	1	38	0	5	0	1	1	1	2	324.2	−0.9	12.629	305	266	26	4.5	1.9	5.0×10^{-11}	10.5
13094	97-310 12:14:50	259	2	3	64	21	23	14	14	14	0	1	1	45	11	5	0	1	1	1	2	324.2	−0.9	11.775	0	314	53	2.5	1.6	1.1×10^{-09}	6.0
13103	97-310 14:25:47	8	2	3	158	20	21	11	8	6	3	1	1	36	1	5	0	1	1	1	2	324.2	−0.9	10.984	228	266	−34	9.7	1.9	9.0×10^{-12}	10.5
13106	97-310 15:08:15	8	3	3	69	22	23	15	7	7	8	0	1	42	0	5	0	1	1	1	2	324.2	−0.9	10.745	353	305	52	12.7	1.9	9.3×10^{-12}	10.5
13108	97-310 18:26:25	8	3	2	118	9	4	10	11	14	12	0	1	2	31	5	0	1	1	1	2	324.2	−0.9	9.789	284	260	10	7.2	1.9	4.6×10^{-13}	10.5
13110	97-310 19:08:53	8	3	3	71	20	21	14	8	8	9	0	1	41	0	5	0	1	1	1	2	324.2	−0.9	9.626	350	301	51	9.7	1.9	9.0×10^{-12}	10.5
13116	97-310 20:33:44	2	2	2	77	12	10	7	12	13	0	1	1	7	11	5	0	1	1	1	2	324.2	−0.9	9.350	342	291	49	4.5	1.9	8.9×10^{-12}	10.5
13120	97-310 20:47:24	2	3	2	151	14	20	9	12	9	6	0	1	36	0	5	0	1	1	1	2	324.2	−0.9	9.310	238	263	−27	9.5	1.7	4.2×10^{-12}	7.6
13121	97-310 20:48:25	79	2	2	93	11	15	2	14	10	14	0	0	20	1	5	0	1	1	1	2	324.2	−0.9	9.307	319	272	36	7.3	3.9	3.5×10^{-12}	128.4
13122	97-310 22:20:00	8	2	2	104	10	14	5	13	15	0	1	1	47	30	5	0	1	1	1	2	324.2	−0.9	9.098	304	265	25	2.3	1.6	1.3×10^{-10}	6.0
13123	97-310 23:58:05	259	2	3	34	21	22	10	9	12	0	1	1	9	28	5	0	1	1	1	2	324.2	−0.9	8.985	42	357	36	7.2	1.9	2.8×10^{-11}	10.5
13124	97-311 03:24:20	8	2	4	104	27	20	28	5	14	12	0	1	47	0	5	0	1	1	1	2	324.2	−0.9	9.136	304	265	25	29.8	1.9	6.1×10^{-13}	10.5
13125	97-311 06:20:57	259	3	3	139	23	27	21	10	8	8	0	1	47	0	5	0	1	1	1	2	324.2	−0.9	9.656	255	260	−13	10.9	2.1	3.1×10^{-11}	14.2
13127	97-311 07:46:12	8	3	4	113	25	20	12	9	14	12	0	1	40	0	5	0	1	1	1	2	324.2	−0.9	10.013	291	262	16	7.2	1.9	3.9×10^{-11}	10.5
13128	97-311 09:32:23	8	2	3	114	20	21	6	8	7	0	1	1	6	8	5	0	1	1	1	2	324.2	−0.9	10.536	290	261	15	9.7	1.9	9.0×10^{-12}	10.5
13134	97-311 17:05:22	22	2	3	106	22	23	6	7	6	0	1	1	39	8	5	0	1	1	1	2	324.2	−0.9	13.354	301	274	22	12.7	1.9	9.3×10^{-12}	10.5
13147	97-312 09:43:19	22	2	3	53	21	26	0	6	5	6	0	0	47	0	5	0	1	1	1	2	324.2	−0.9	20.341	15	6	42	32.6	1.6	4.7×10^{-13}	6.0
13152	97-314 22:49:36	22	2	2	162	12	5	6	11	15	0	1	1	36	30	5	0	1	1	1	2	324.4	−0.9	41.172	222	269	−38	7.2	1.9	8.6×10^{-13}	10.5
13153	97-315 02:00:42	259	3	5	203	54	56	30	15	14	7	0	1	1	1	5	0	1	1	1	2	324.5	−0.9	42.057	165	336	−53	2.5	1.6	2.5×10^{-07}	6.0
13174	97-345 04:52:39	22	2	2	117	10	15	0	10	11	6	0	0	38	0	5	0	1	1	1	2	327.4	−0.9	48.295	285	264	12	14.0	1.6	5.5×10^{-13}	6.0
13408	97-349 14:20:50	8	3	2	139	8	10	10	11	12	7	0	1	3	31	5	0	1	1	1	2	327.7	−1.0	13.173	255	263	−13	9.2	1.6	5.1×10^{-13}	6.0
13409	97-349 14:35:00	8	3	5	101	49	49	24	10	9	9	0	1	47	0	5	0	1	1	1	2	327.7	−1.0	13.076	308	270	29	11.8	11.8	2.7×10^{-10}	5858.3
13411	97-349 16:42:23	8	3	2	189	10	14	7	13	14	5	0	1	5	31	5	0	1	1	1	2	327.7	−1.0	12.220	184	311	−55	2.7	1.6	6.7×10^{-11}	6.0
13424	97-349 21:39:40	8	3	3	119	21	25	18	8	12	10	0	1	44	0	5	0	1	1	1	2	327.7	−1.0	10.416	283	263	9	5.6	1.6	1.1×10^{-10}	6.0
13425	97-349 23:32:55	8	3	4	113	24	27	20	9	9	5	0	1	44	8	5	0	1	1	1	2	327.7	−1.0	9.849	291	265	16	12.1	1.6	2.9×10^{-11}	6.0
13428	97-350 05:12:39	8	2	4	68	26	22	13	13	13	0	1	1	11	30	5	0	1	1	1	2	327.7	−1.0	8.840	354	310	53	2.0	1.9	5.5×10^{-09}	10.5
13433	97-350 11:56:41	2	2	2	88	11	14	5	13	14	1	1	1	3	29	5	0	1	1	1	2	327.7	−1.0	9.431	326	280	42	2.7	1.6	7.8×10^{-11}	6.0
13435	97-350 12:02:14	2	3	2	119	12	14	5	12	13	8	0	1	5	28	5	0	1	1	1	2	327.7	−1.0	9.452	283	263	9	5.9	1.6	7.4×10^{-12}	6.0
13436	97-350 12:02:43	1	2	2	102	9	10	0	11	12	8	0	0	3	30	5	0	1	1	1	2	327.7	−1.0	9.454	307	269	28	7.2	1.9	1.2×10^{-12}	10.5
13437	97-350 12:03:13	2	2	2	146	8	4	3	12	15	15	0	1	3	0	5	0	1	1	1	2	327.7	−1.0	9.456	245	265	−20	4.5	1.9	1.7×10^{-12}	10.5
13439	97-35012:06:50	2	2	4	143	25	27	20	14	13	15	1	1	15	11	5	0	1	1	1	2	327.7	−1.0	9.470	249	264	−17	2.5	1.6	4.1×10^{-09}	6.0
13441	97-350 12:08:37	2	3	2	87	10	4	6	12	14	11	0	1	6	0	5	0	1	1	1	2	327.7	−1.0	9.476	328	281	43	4.5	1.9	2.4×10^{-12}	10.5
13445	97-350 15:39:31	22	2	4	142	26	22	21	10	7	0	1	1	17	14	5	0	1	1	1	2	327.7	−1.0	10.428	250	264	−16	4.5	1.9	2.9×10^{-10}	10.5
13447	97-350 17:22:40	259	3	5	107	52	49	25	9	10	5	0	1	63	0	5	0	1	1	1	2	327.7	−1.0	11.012	300	267	23	7.2	1.9	1.8×10^{-09}	10.5
13448	97-350 19:11:52	22	3	4	113	26	28	6	7	7	5	0	1	47	0	5	0	1	1	1	2	327.7	−1.0	11.689	291	265	16	19.9	1.6	9.2×10^{-12}	6.0
13449	97-350 20:15:34	22	2	3	176	19	14	9	12	15	0	1	1	45	30	5	0	1	1	1	2	327.7	−1.0	12.106	203	288	−50	2.0	1.9	7.8×10^{-10}	10.5
13451	97-351 04:02:42	22	3	3	148	23	22	7	14	15	10	0	1	6	1	5	0	1	1	1	2	327.7	−1.0	15.426	242	265	−23	2.0	1.9	3.5×10^{-09}	10.5
13452	97-352 09:03:50	22	3	3	135	22	26	5	5	5	5	0	1	46	0	5	0	1	1	1	2	327.8	−1.0	27.675	260	263	−8	40.9	1.6	2.4×10^{-13}	6.0

Table 3 (*continued*)

No.	IMP. DATE	TEV	CLN	AR	SEC	IA	EA	CA	IT	ET	EIT	EIC	ICC	PA	PET	EVD	ICP	ECP	CCP	PCP	HV	LON	LAT	D_{Jup}	ROT	S_{LON}	S_{LAT}	V	VEF	M	MEF
13459	98-041 19:22:17	259	3	2	123	12	19	10	11	11	8	0	1	37	0	5	0	1	1	1	1	332.8	−1.0	9.188	277	276	5	7.2	1.9	5.6×10^{-12}	10.5
13460	98-041 19:23:18	259	3	2	134	11	13	5	11	12	7	0	1	3	23	5	0	1	1	1	1	332.8	−1.0	9.185	262	276	−6	9.2	1.6	1.4×10^{-12}	6.0
13461	98-041 19:24:18	259	3	2	155	13	20	3	12	10	8	0	1	38	0	5	0	1	1	1	1	332.8	−1.0	9.182	232	282	−30	4.5	1.9	3.5×10^{-11}	10.5
13462	98-041 23:41:08	259	3	3	109	20	22	9	7	8	10	0	1	39	0	5	0	1	1	1	1	332.8	−1.0	8.863	297	279	21	18.3	1.6	1.8×10^{-12}	6.0
13464	98-042 08:18:38	259	2	5	121	50	13	7	9	0	5	0	1	62	0	5	0	1	1	1	1	332.7	−1.0	10.600	280	277	8	7.2	1.9	7.7×10^{-11}	10.5
13465	98-042 12:37:40	259	3	2	110	13	20	5	12	10	6	0	1	39	9	5	0	1	1	1	1	332.7	−1.0	12.211	295	279	20	4.5	1.9	3.5×10^{-11}	10.5
13466	98-042 12:37:40	259	3	4	174	27	49	12	6	10	5	0	1	47	0	5	0	1	1	1	1	332.7	−1.0	12.211	205	299	−47	19.0	1.9	2.8×10^{-11}	10.5
13467	98-081 12:46:52	259	3	2	39	12	49	3	11	9	6	0	1	27	1	5	0	1	1	1	2	336.5	−1.1	59.297	35	21	41	7.2	1.9	5.5×10^{-11}	10.5
13605	98-087 15:18:29	22	2	2	176	8	10	8	13	14	0	1	1	8	12	5	0	1	1	1	2	336.9	−1.1	13.535	203	313	−49	2.7	1.6	2.5×10^{-11}	6.0
13609	98-087 17:47:06	22	3	4	105	24	28	24	8	9	9	0	1	47	0	5	0	1	1	1	2	336.9	−1.1	12.499	302	292	25	14.0	1.6	2.3×10^{-11}	6.0
13613	98-087 20:15:44	22	2	2	235	9	19	4	11	11	12	0	0	15	0	5	0	1	1	1	2	336.9	−1.1	11.516	120	34	−23	7.2	1.9	3.5×10^{-12}	10.5
13622	98-088 07:13:58	22	2	2	111	12	15	6	15	14	0	1	1	40	13	5	0	1	1	1	2	336.9	−1.1	8.849	294	290	19	2.5	1.6	1.4×10^{-10}	6.0
13627	98-088 13:29:57	2	2	2	110	8	9	2	13	13	0	1	1	3	0	5	0	1	1	1	2	336.9	−1.1	9.524	295	290	20	2.3	1.9	4.1×10^{-11}	10.5
13630	98-088 15:47:24	22	2	3	154	23	5	18	9	14	15	0	1	3	0	5	0	1	1	1	2	336.9	−1.1	10.136	233	293	−29	7.2	1.9	3.7×10^{-12}	10.5
13631	98-089 04:10:34	22	3	3	126	22	25	14	6	9	9	0	1	45	0	5	0	1	1	1	2	336.9	−1.1	15.080	273	287	2	19.6	1.6	3.2×10^{-12}	6.0
13632	98-089 04:31:48	22	3	4	12	27	31	17	14	13	6	0	1	35	31	5	0	1	1	1	2	336.9	−1.1	15.237	73	36	13	2.0	1.9	2.6×10^{-08}	10.5
13634	98-089 19:02:23	22	2	2	199	9	13	0	13	14	13	0	0	46	5	5	0	1	1	1	2	336.9	−1.1	21.660	170	356	−54	2.7	1.6	4.8×10^{-11}	6.0
13638	98-101 03:00:41	259	2	2	51	14	11	5	11	15	0	1	1	39	30	5	0	1	1	1	2	338.0	−1.1	88.898	18	10	50	7.2	1.9	3.3×10^{-12}	10.5
13852	98-151 11:51:41	8	2	2	104	10	13	4	14	13	9	0	0	38	0	5	0	1	1	1	2	342.7	−1.2	12.741	304	305	26	3.9	1.6	1.6×10^{-11}	6.0
13865	98-151 16:34:47	8	2	2	43	9	21	3	15	11	5	0	0	8	26	5	0	1	1	1	2	342.7	−1.2	10.889	30	28	44	2.0	1.9	4.2×10^{-10}	10.5
13871	98-151 17:31:24	8	2	3	102	21	23	4	8	7	9	0	0	45	0	5	0	1	1	1	2	342.7	−1.2	10.563	307	306	28	17.4	1.6	2.9×10^{-12}	6.0
13877	98-151 19:03:26	8	3	4	127	25	29	24	8	9	6	0	1	47	0	5	0	1	1	1	2	342.7	−1.2	10.076	271	299	0	14.0	1.6	3.1×10^{-11}	6.0
13885	98-151 20:14:13	8	2	3	165	21	24	10	7	6	2	1	1	41	1	5	0	1	1	1	2	342.7	−1.2	9.747	218	311	−41	21.6	1.6	1.4×10^{-12}	6.0
13887	98-151 20:35:27	8	2	2	147	8	9	0	12	13	8	0	0	8	31	5	0	1	1	1	2	342.7	−1.2	9.657	243	301	−22	4.5	1.9	3.9×10^{-12}	10.5
13892	98-151 21:17:20	2	3	2	136	8	11	2	12	13	6	0	1	2	31	5	0	1	1	1	2	342.7	−1.2	9.490	259	299	−10	5.9	1.6	2.3×10^{-12}	6.0
13910	98-153 05:34:11	22	3	4	35	29	30	11	9	10	6	0	1	47	0	5	0	1	1	1	2	342.7	−1.2	18.087	41	36	37	7.2	1.9	3.6×10^{-10}	10.5
14072	98-201 16:04:38	8	3	3	151	20	23	12	8	8	10	0	1	40	0	5	0	1	1	1	2	347.2	−1.2	10.303	238	307	−26	16.0	1.6	3.5×10^{-12}	6.0
14075	98-201 18:53:29	259	3	4	120	29	49	17	8	10	5	0	1	47	0	5	0	1	1	1	2	347.2	−1.2	9.517	281	303	8	9.7	1.9	2.6×10^{-10}	10.5
14076	98-204 14:05:27	259	3	2	155	11	49	3	10	9	7	0	1	27	1	5	0	1	1	1	2	347.3	−1.2	32.483	232	308	−30	9.7	1.9	2.0×10^{-11}	10.5
14292	98-268 15:32:26	15	2	2	11	15	3	3	0	3	11	0	0	43	31	5	0	1	1	1	2	353.3	−1.2	13.757	75	43	12	11.8	11.8	2.7×10^{-13}	5858.3
14293	98-268 15:39:31	8	2	2	87	12	19	10	14	13	3	1	1	38	0	5	0	1	1	1	2	353.3	−1.2	13.706	328	312	43	2.0	1.9	4.8×10^{-10}	10.5
14313	98-268 18:50:36	8	3	2	127	11	49	3	11	10	7	0	1	27	1	5	0	1	1	1	2	353.3	−1.2	12.355	271	294	0	7.2	1.9	4.7×10^{-11}	10.5
14324	98-268 21:33:23	8	3	2	31	13	49	4	10	10	7	0	1	27	1	5	0	1	1	1	2	353.3	−1.3	11.287	46	34	33	9.7	1.9	2.8×10^{-11}	10.5
14326	98-268 22:15:51	8	3	2	134	11	14	17	11	12	6	0	1	37	0	5	0	1	1	1	2	353.3	−1.3	11.026	262	294	−7	9.2	1.6	1.6×10^{-12}	6.0
14329	98-268 23:19:34	8	3	2	157	9	11	3	12	13	9	0	1	3	4	5	0	1	1	1	2	353.3	−1.3	10.654	229	301	−32	5.9	1.6	2.8×10^{-12}	6.0
14332	98-269 00:02:01	8	3	3	127	22	25	23	7	7	8	0	1	44	0	5	0	1	1	1	2	353.3	−1.3	10.419	271	294	0	19.9	1.6	3.0×10^{-12}	6.0

14335	98-269 00:30:20	8	3	4	121	24	28	25	7	9	9	0	1	46	0	5	0	1	1	1	2	353.3	−1.3	10.270	280	294	7	16.0	1.6	1.6×10^{-11}	6.0
14337	98-269 02:09:26	8	2	2	121	13	4	6	12	15	15	0	1	3	31	5	0	1	1	1	2	353.3	−1.3	9.795	280	294	7	4.5	1.9	3.9×10^{-12}	10.5
14351	98-269 08:45:48	8	3	2	134	9	13	9	13	14	8	0	1	6	23	5	0	1	1	1	2	353.3	−1.3	8.913	262	294	−7	2.7	1.6	4.8×10^{-11}	6.0
14352	98-269 09:14:06	8	3	2	233	12	52	3	10	14	11	0	1	27	0	5	0	1	1	1	2	353.3	−1.3	8.925	122	40	−26	9.7	1.9	4.0×10^{-11}	10.5
14359	98-269 20:26:29	22	2	2	163	8	11	0	12	13	6	0	0	3	30	5	0	1	1	1	2	353.3	−1.3	11.721	221	305	−38	5.9	1.6	2.3×10^{-12}	6.0
14360	98-269 21:30:11	22	3	2	154	13	20	5	13	11	11	0	1	36	0	5	0	1	1	1	2	353.3	−1.3	12.142	233	299	−29	2.3	1.9	3.7×10^{-10}	10.5
14361	98-269 23:37:35	22	3	4	115	28	31	14	6	8	5	0	1	47	0	5	0	1	1	1	2	353.3	−1.3	13.019	288	296	14	19.0	1.9	2.3×10^{-11}	10.5
14362	98-270 00:20:03	22	3	3	142	21	23	10	7	7	9	0	1	40	0	5	0	1	1	1	2	353.3	−1.3	13.319	250	295	−16	19.9	1.6	1.7×10^{-12}	6.0
14364	98-270 07:03:29	22	2	4	35	24	22	21	10	9	0	1	1	47	16	5	0	1	1	1	2	353.3	−1.3	16.267	41	31	37	4.5	1.9	2.1×10^{-10}	10.5
14365	98-271 05:42:24	22	3	3	93	23	8	13	15	11	14	0	1	26	5	5	0	1	1	1	2	353.3	−1.3	25.931	319	307	37	2.0	1.9	5.4×10^{-10}	10.5
14367	98-271 22:41:37	22	2	3	54	20	21	17	11	9	2	1	1	17	11	5	0	1	1	1	2	353.4	−1.3	32.410	14	7	51	2.3	1.9	9.7×10^{-10}	10.5
14373	98-278 00:03:28	259	2	2	20	9	15	0	11	12	12	0	0	18	1	5	0	1	1	1	2	353.9	−1.2	70.485	62	40	22	9.2	1.6	1.3×10^{-12}	6.0
14437	98-325 02:06:29	22	2	2	234	12	4	3	15	14	11	0	0	5	31	5	0	1	1	1	2	358.5	−1.3	19.262	121	40	−25	2.0	1.9	6.3×10^{-11}	10.5
14464	98-325 11:39:47	22	3	2	132	11	50	5	12	10	7	0	1	28	1	5	0	1	1	1	2	358.5	−1.3	15.047	264	294	−4	4.5	1.9	2.9×10^{-10}	10.5
14491	98-325 17:40:46	8	2	2	158	8	12	3	11	12	4	0	0	36	0	5	0	1	1	1	2	358.5	−1.3	12.471	228	301	−33	9.2	1.6	7.0×10^{-13}	6.0
14502	98-325 19:19:51	8	3	3	141	21	23	18	8	8	8	0	1	43	0	5	0	1	1	1	2	358.5	−1.3	11.810	252	295	−15	16.0	1.6	4.0×10^{-12}	6.0
14509	98-325 23:13:26	8	3	3	164	21	23	8	7	7	9	0	1	44	0	5	0	1	1	1	2	358.5	−1.3	10.414	219	306	−39	19.9	1.6	1.7×10^{-12}	6.0
14510	98-325 23:15:26	259	2	2	70	10	12	4	15	15	1	1	1	37	12	5	0	1	1	1	2	358.5	−1.3	10.403	352	337	53	2.1	1.6	1.2×10^{-10}	6.0
14511	98-325 23:20:29	8	2	2	157	8	10	7	14	13	3	1	1	2	31	5	0	1	1	1	2	358.5	−1.3	10.377	229	301	−32	3.9	1.6	7.1×10^{-12}	6.0
14513	98-326 00:45:25	8	3	3	137	21	23	20	9	8	6	0	1	43	0	5	0	1	1	1	2	358.5	−1.3	9.955	257	294	−10	13.8	1.6	6.1×10^{-12}	6.0
14515	98-326 02:17:26	8	3	4	147	28	49	23	9	10	7	0	1	47	0	5	0	1	1	1	2	358.5	−1.3	9.567	243	296	−22	7.2	1.9	5.1×10^{-10}	10.5
14516	98-326 17:10:15	259	3	3	153	21	22	8	7	7	5	0	1	10	0	5	0	1	1	1	2	358.5	−1.3	10.854	235	299	−28	12.7	1.9	6.3×10^{-12}	10.5
14518	98-327 00:13:17	259	3	2	69	11	49	5	12	10	7	0	1	26	1	5	0	1	1	1	2	358.5	−1.3	13.676	353	339	53	4.5	1.9	2.1×10^{-10}	10.5
14520	98-327 23:22:10	259	2	3	245	19	23	5	11	8	15	0	1	47	0	5	0	1	1	1	2	358.5	−1.3	23.879	105	43	−13	7.8	3.5	2.1×10^{-11}	85.4
14538	99-017 19:09:53	259	2	3	134	22	21	11	7	15	0	1	1	22	31	5	0	1	1	1	2	3.7	−1.3	96.652	262	300	−7	12.7	1.9	6.7×10^{-12}	10.5
14570	99-029 23:01:19	22	2	2	96	8	4	4	15	14	11	0	0	3	31	5	0	1	1	1	2	4.9	−1.3	29.833	315	313	34	2.0	1.9	3.3×10^{-11}	10.5
14656	99-031 12:10:48	22	2	2	150	11	13	5	14	14	0	1	1	44	17	5	0	1	1	1	2	5.0	−1.3	14.030	239	306	−25	2.5	1.6	8.7×10^{-11}	6.0
14659	99-031 12:53:16	22	3	2	227	11	49	6	12	10	7	0	1	27	1	5	0	1	1	1	2	5.0	−1.3	13.724	131	45	−32	4.5	1.9	2.1×10^{-10}	10.5
14678	99-031 21:44:06	22	3	2	90	8	11	3	12	13	5	0	1	2	31	5	0	1	1	1	2	5.0	−1.3	10.339	323	318	40	5.9	1.6	2.3×10^{-12}	6.0
14683	99-031 23:03:59	85	2	2	51	13	52	3	10	9	6	0	0	27	1	5	0	1	1	1	2	5.0	−1.3	9.961	18	21	50	9.7	1.9	4.7×10^{-11}	10.5
14685	99-032 00:12:44	2	3	4	68	29	49	27	8	10	9	0	1	47	0	5	0	1	1	1	2	5.0	−1.3	9.679	354	350	53	9.7	1.9	2.6×10^{-10}	10.5
14688	99-032 01:37:40	22	2	6	168	56	22	24	15	11	0	1	1	60	30	5	0	1	1	1	2	5.0	−1.3	9.397	214	318	−43	2.0	1.9	5.0×10^{-08}	10.5
14689	99-032 01:57:13	2	3	5	87	49	49	27	10	10	9	0	1	47	0	5	0	1	1	1	2	5.0	−1.3	9.343	328	321	43	11.8	11.8	2.7×10^{-10}	5858.3
14692	99-032 02:06:18	2	3	2	115	12	19	7	13	13	8	0	1	2	0	5	0	1	1	1	2	5.0	−1.3	9.320	288	304	14	2.3	1.9	2.6×10^{-10}	10.5
14693	99-032 02:12:22	2	3	3	123	21	23	13	8	9	9	0	1	5	31	5	0	1	1	1	2	5.0	−1.3	9.305	277	303	5	14.0	1.6	5.9×10^{-12}	6.0
14699	99-032 02:28:47	2	3	3	117	20	22	15	9	9	8	0	1	39	0	5	0	1	1	1	2	5.0	−1.3	9.267	285	304	12	12.1	1.6	6.3×10^{-12}	6.0
14700	99-032 03:16:21	259	3	2	0	13	22	10	11	12	12	0	1	35	0	5	0	1	1	1	2	5.0	−1.3	9.185	999	999	999	7.2	1.9	1.1×10^{-11}	10.5
14701	99-032 04:17:26	259	3	4	0	30	31	27	8	8	5	0	1	47	0	5	0	1	1	1	2	5.0	−1.3	9.123	999	999	999	9.7	1.9	2.1×10^{-10}	10.5
14702	99-032 04:17:26	259	3	2	0	14	20	9	12	14	12	0	1	3	31	5	0	1	1	1	2	5.0	−1.3	9.123	999	999	999	3.8	1.6	7.0×10^{-11}	6.0
14705	99-032 08:36:16	259	3	2	167	12	20	10	13	12	9	0	1	36	0	5	0	1	1	1	2	5.0	−1.3	9.410	215	317	−42	2.3	1.9	3.1×10^{-10}	10.5

Table 3 (*continued*)

No.	IMP. DATE	TEV	CLN	AR	SEC	IA	EA	CA	IT	ET	EIT	EIC	ICC	PA	PET	EVD	ICP	ECP	CCP	PCP	HV	LON	LAT	D_{Jup}	ROT	S_{LON}	S_{LAT}	V	VEF	M	MEF
14706	99-032 08:36:16	259	3	3	0	22	27	7	6	5	5	0	1	46	0	5	0	1	1	1	2	5.0	−1.3	9.410	999	999	999	32.6	1.6	6.9×10^{-13}	6.0
14707	99-032 17:13:58	259	3	2	0	13	49	9	11	10	7	0	1	27	1	5	0	1	1	1	2	5.0	−1.3	12.015	999	999	999	7.2	1.9	6.6×10^{-11}	10.5
14708	99-033 01:51:26	259	3	4	0	25	30	14	8	6	5	0	1	47	0	5	0	1	1	1	2	5.0	−1.3	15.745	999	999	999	18.9	1.6	1.3×10^{-11}	6.0
14709	99-034 08:03:21	259	3	3	0	23	26	15	7	8	6	0	1	47	0	5	0	1	1	1	2	5.0	−1.3	28.881	999	999	999	18.3	1.6	6.0×10^{-12}	6.0
14716	99-102 02:27:38	259	2	2	42	11	19	12	14	15	15	0	1	8	2	5	0	1	1	1	2	11.3	−1.3	124.413	31	53	46	2.0	1.9	4.0×10^{-10}	10.5
14805	99-123 05:16:47	22	2	2	107	11	4	3	15	14	11	0	0	17	0	5	0	1	1	1	2	13.4	−1.3	11.965	300	328	21	2.0	1.9	5.3×10^{-11}	10.5
14826	99-123 10:35:16	22	3	2	152	11	13	4	12	13	7	0	1	2	31	5	0	1	1	1	2	13.4	−1.3	10.247	236	326	−29	5.9	1.6	5.3×10^{-12}	6.0
14847	99-124 00:23:22	22	2	2	78	12	4	3	15	14	11	0	0	3	13	5	0	1	1	1	2	13.4	−1.3	10.508	340	355	47	2.0	1.9	6.3×10^{-11}	10.5
14856	99-124 02:52:01	22	2	2	95	11	6	8	13	15	0	1	1	44	30	5	0	1	1	1	2	13.4	−1.3	11.291	316	336	33	2.3	1.9	4.1×10^{-11}	10.5
14874	99-124 15:57:38	22	2	2	106	8	13	0	15	15	7	0	0	18	26	5	0	1	1	1	2	13.4	−1.3	16.719	301	329	22	2.1	1.6	1.1×10^{-10}	6.0
14905	99-126 08:51:37	259	2	2	40	11	14	0	14	15	12	0	0	10	6	5	0	1	1	1	2	13.4	−1.3	33.599	34	54	39	2.1	1.6	2.0×10^{-10}	6.0
14974	99-182 00:20:05	22	2	2	121	15	6	3	0	0	10	0	0	6	31	5	0	1	1	1	2	18.8	−1.3	19.057	280	334	7	11.8	11.8	4.4×10^{-13}	5858.3
15003	99-182 08:28:27	22	2	2	146	15	15	6	0	0	0	1	1	4	26	5	0	1	1	1	2	18.8	−1.3	15.193	245	336	−20	11.8	11.8	1.8×10^{-12}	5858.3
15005	99-182 08:49:41	22	2	2	139	15	7	3	0	14	7	0	1	5	31	5	0	1	1	1	2	18.8	−1.3	15.020	255	334	−12	11.8	11.8	5.2×10^{-13}	5858.3
15040	99-182 14:57:45	8	2	2	123	15	7	5	0	15	15	0	1	4	20	5	0	1	1	1	2	18.8	−1.3	12.016	277	333	5	11.8	11.8	5.2×10^{-13}	5858.3
15045	99-182 15:26:03	8	2	2	150	15	6	3	0	14	12	0	1	5	31	5	0	1	1	1	2	18.8	−1.3	11.787	239	337	−25	11.8	11.8	4.4×10^{-13}	5858.3
15076	99-18218:30:04	8	2	2	83	14	5	8	4	15	15	0	1	4	3	5	0	1	1	1	2	18.8	−1.3	10.334	333	356	46	70.0	1.9	4.7×10^{-16}	10.5
15080	99-182 18:51:18	8	2	2	60	8	14	2	12	12	6	0	0	1	1	5	0	1	1	1	2	18.8	−1.3	10.172	6	36	53	7.3	1.6	1.9×10^{-12}	6.0
15106	99-182 21:05:48	8	2	2	29	8	19	5	12	12	11	0	0	47	1	5	0	1	1	1	2	18.9	−1.3	9.196	49	75	32	4.5	1.9	1.3×10^{-11}	10.5
15119	99-182 23:13:11	8	2	2	173	8	20	3	11	14	11	0	0	10	0	5	0	1	1	1	2	18.9	−1.3	8.387	207	355	−47	7.2	1.9	3.5×10^{-12}	10.5
15129	99-183 00:23:57	8	2	6	237	57	11	25	13	0	4	1	1	28	1	5	0	1	1	1	2	18.9	−1.3	8.008	117	80	−21	2.0	1.9	1.5×10^{-08}	10.5
15140	99-183 03:42:08	8	2	2	196	8	12	0	12	12	5	0	0	5	1	5	0	1	1	1	2	18.9	−1.3	7.339	174	36	−55	7.3	1.6	1.4×10^{-12}	6.0
15215	99-183 20:55:30	8	2	4	90	26	29	15	9	6	0	1	1	47	6	5	0	1	1	1	2	18.8	−1.3	12.857	323	348	40	16.3	1.9	2.3×10^{-11}	10.1
15219	99-183 22:06:16	8	3	2	68	13	49	10	12	11	7	0	1	26	1	5	0	1	1	1	2	18.8	−1.3	13.435	354	20	53	4.5	1.9	2.9×10^{-10}	10.5
15225	99-184 04:42:38	8	3	2	2	14	52	9	11	9	6	0	1	26	1	5	0	1	1	1	2	18.8	−1.3	16.646	87	83	2	7.2	1.9	1.3×10^{-10}	10.5
15231	99-185 02:39:05	22	3	2	183	11	50	6	12	10	7	0	1	28	1	5	0	1	1	1	2	18.9	−1.3	26.284	193	8	−52	4.5	1.9	2.9×10^{-10}	10.5
15233	99-186 09:26:23	22	3	3	138	20	23	2	10	9	5	0	1	44	0	5	0	1	1	1	2	18.9	−1.3	37.338	256	334	−11	9.5	1.7	1.3×10^{-11}	7.6
15234	99-189 01:29:37	22	2	3	247	23	26	15	12	13	0	1	1	47	10	5	0	1	1	1	2	19.1	−1.3	54.587	103	83	−10	2.5	1.6	2.6×10^{-09}	6.0
15282	99-223 16:52:46	8	2	2	100	12	20	4	15	14	11	0	0	22	0	5	0	1	1	1	2	22.6	−1.3	13.962	309	346	30	2.0	1.9	5.7×10^{-10}	10.5
15343	99-223 23:43:16	8	3	2	216	13	49	6	11	11	7	0	1	26	1	5	0	1	1	1	2	22.6	−1.3	10.662	146	72	−43	7.2	1.9	6.6×10^{-11}	10.5
15347	99-224 00:18:39	8	2	2	82	12	20	3	15	14	11	0	0	37	0	5	0	1	1	1	2	22.6	−1.3	10.390	335	2	47	2.0	1.9	5.7×10^{-10}	10.5
15425	99-224 14:35:05	8	3	2	79	14	31	7	10	9	6	0	1	27	0	5	0	1	1	1	2	22.6	−1.3	7.760	339	6	49	9.7	1.9	2.3×10^{-11}	10.5
15433	99-224 16:00:00	8	2	2	12	8	20	11	0	14	11	0	1	25	0	5	0	1	1	1	2	22.6	−1.3	8.146	73	86	13	11.8	11.8	9.3×10^{-13}	5858.3
15451	99-224 20:50:11	8	2	2	11	11	6	9	1	15	4	1	1	37	31	5	0	1	1	1	2	22.6	−1.3	10.022	75	87	12	70.0	1.9	3.5×10^{-16}	10.5
15474	99-225 02:22:50	8	3	2	235	14	50	11	12	11	6	0	1	27	1	5	0	1	1	1	2	22.6	−1.3	12.642	120	85	−24	4.5	1.9	4.8×10^{-10}	10.5

15507	99-225 16:03:53	8	2	2	54	12	15	8	11	0	6	0	1	26	1	5	0	1	1	1	2	22.6	−1.3	19.186	14	52	51	7.2	1.9	4.3×10^{-12}	10.5
15561	99-254 04:10:07	259	2	2	7	8	13	4	11	12	11	0	0	5	28	5	0	1	1	1	2	25.3	−1.2	40.413	80	87	7	9.2	1.6	8.3×10^{-13}	6.0
15564	99-256 19:09:39	22	2	2	111	11	12	4	15	15	6	0	0	20	30	5	0	1	1	1	2	25.6	−1.3	17.213	294	341	19	2.0	1.9	2.0×10^{-10}	10.5
15577	99-257 01:18:28	8	2	2	179	10	13	5	15	15	14	0	0	2	25	5	0	1	1	1	2	25.6	−1.3	14.173	198	8	−51	2.1	1.6	1.5×10^{-10}	6.0
15583	99-257 02:50:30	8	2	2	189	8	31	3	12	10	7	0	0	28	1	5	0	1	1	1	2	25.7	−1.3	13.392	184	27	−55	4.5	1.9	8.9×10^{-11}	10.5
15672	99-258 18:00:19	22	2	2	20	11	15	0	15	1	10	0	0	37	31	5	0	1	1	1	2	25.7	−1.3	15.867	62	84	22	11.8	9.5	9.7×10^{-13}	2690.1
15682	99-259 06:02:14	22	3	3	82	21	24	14	10	13	12	0	1	47	2	5	0	1	1	1	2	25.7	−1.3	21.482	335	2	47	3.8	1.6	3.0×10^{-10}	6.0
15693	99-259 15:42:37	8	2	2	108	12	19	9	13	13	0	1	1	40	2	5	0	1	1	1	2	25.7	−1.3	25.549	298	342	22	2.3	1.9	2.6×10^{-10}	10.5
15699	99-259 21:43:36	8	2	2	45	8	11	0	11	10	11	0	0	2	27	5	0	1	1	1	2	25.7	−1.3	27.871	27	65	46	13.8	1.6	2.2×10^{-13}	6.0
15702	99-260 01:44:14	22	3	2	91	14	21	9	13	10	7	0	1	40	5	5	0	1	1	1	2	25.7	−1.3	29.329	322	352	39	2.3	1.9	5.2×10^{-10}	10.5
15719	99-284 07:44:58	8	2	2	159	15	20	0	0	12	13	0	0	8	0	5	0	1	1	1	2	28.1	−1.2	7.176	226	342	−35	3.2	2.0	1.4×10^{-10}	12.5
15734	99-285 03:16:20	8	2	2	103	10	13	0	15	15	14	0	0	20	29	5	0	1	1	1	2	28.1	−1.2	17.966	305	342	26	2.1	1.6	1.5×10^{-10}	6.0
15739	99-285 22:40:38	22	2	2	31	8	14	0	12	14	11	0	0	8	2	5	0	1	1	1	2	28.1	−1.2	27.021	46	74	32	3.8	1.6	1.5×10^{-11}	6.0
15743	99-294 09:07:04	22	2	2	134	8	14	0	12	13	10	0	0	2	26	5	0	1	1	1	2	28.6	−1.2	77.026	262	335	−8	5.9	1.6	3.8×10^{-12}	6.0
15749	99-315 15:34:38	259	3	3	79	21	25	9	9	15	6	0	1	45	0	5	0	1	1	1	3	30.6	−1.2	88.770	339	360	46	4.8	1.6	1.7×10^{-10}	6.0
15750	99-327 16:37:12	259	2	2	39	9	12	0	14	15	14	0	0	8	6	5	0	1	1	1	3	32.0	−1.2	32.266	35	62	39	2.1	1.6	1.1×10^{-10}	6.0
15763	99-329 08:54:46	8	2	2	185	10	13	2	15	15	6	0	0	10	30	5	0	1	1	1	3	32.2	−1.2	13.797	190	10	−57	2.1	1.6	1.5×10^{-10}	6.0
15777	99-329 12:20:02	8	3	2	40	13	49	7	12	12	6	0	1	26	1	5	0	1	1	1	3	32.3	−1.2	11.862	34	61	40	4.5	1.9	2.9×10^{-10}	10.5
15835	99-330 06:03:43	8	2	2	195	15	20	0	0	15	14	0	0	7	0	5	0	1	1	1	3	32.3	−1.2	6.548	176	32	−58	3.2	2.0	1.4×10^{-10}	12.5
15838	99-330 09:19:53	259	3	3	127	23	27	14	8	9	7	0	1	46	0	5	0	1	1	1	3	32.3	−1.2	8.118	271	330	0	14.0	1.6	1.7×10^{-11}	6.0
15840	99-330 12:40:05	8	3	2	152	10	13	10	14	15	11	0	1	41	12	5	0	1	1	1	3	32.3	−1.2	9.975	236	333	−29	2.1	1.6	1.5×10^{-10}	6.0
15841	99-330 17:57:34	259	3	2	217	14	49	13	12	12	6	0	1	26	1	5	0	1	1	1	3	32.3	−1.2	12.977	145	67	−44	4.5	1.9	3.4×10^{-10}	10.5
15842	99-331 00:13:41	8	3	4	127	28	49	25	9	12	5	0	1	47	0	5	0	1	1	1	3	32.3	−1.2	16.371	271	330	0	7.2	1.9	5.1×10^{-10}	10.5
15846	99-346 22:13:33	259	2	4	67	31	50	27	14	15	0	1	1	26	11	5	0	1	1	1	4	33.4	−1.2	86.083	356	20	51	2.0	1.9	9.7×10^{-08}	10.5

value allowed by the instrument electronics is 48 (Paper I). This is also inherent in all Galileo and Ulysses data sets published earlier (Papers II to VII) and it is due to a bit flip. According to our present understanding the correct PA values are obtained by subtracting 32 from all entries which have values between 49 and 63. Values of 48 and lower should remain unchanged.

4. Analysis

The positive charge measured on the ion collector, Q_I, is the most important impact parameter determined by DDS because it is rather insensitive to noise. Fig. 5 shows the distribution of Q_I for the full 1997–1999 data set (small and big particles together). Ion impact charges have been detected over the entire range of six orders of magnitude the instrument can measure. The maximum measured charge was $Q_I = 3 \times 10^{-9}$ C, well below the saturation limit of $\sim 10^{-8}$ C. The impact charge distribution of the big particles ($Q_I > 10^{-13}$ C) follows a power law with index -0.37 and is shown as a dashed line. This slope is close to the value of -0.31 derived for the jovian system from the 1996 Galileo data set (Paper VI). It is also close to the Galileo value of $-\frac{1}{3}$ given in Paper II for the inner solar system. Values derived for the outer solar system are somewhat steeper: $-\frac{1}{2}$ (Ulysses, Paper III) and -0.43 (Galileo, Paper IV), respectively. Note that the jovian stream particles (AR1) were excluded from the power law fit.

In Fig. 5 the small stream particles ($Q_I < 10^{-13}$ C) occur in only two histogram bins. To investigate their behaviour in more detail we show their number per individual digital step separately in Fig. 6. The distribution flattens for impact charges below 3×10^{-14} C. This indicates that the sensitivity threshold of DDS may not be sharp. The impact charge distribution for small particles with $Q_I > 3 \times 10^{-14}$ C follows a power law with index -3.6. Although it is somewhat flatter than the slope found from the 1996 Galileo data set (-4.5, Paper VI) it indicates that the size distribution of the stream particles rises strongly towards smaller particles. Note that the distribution of the stream particles is much steeper than that of the big particles shown in Fig. 5.

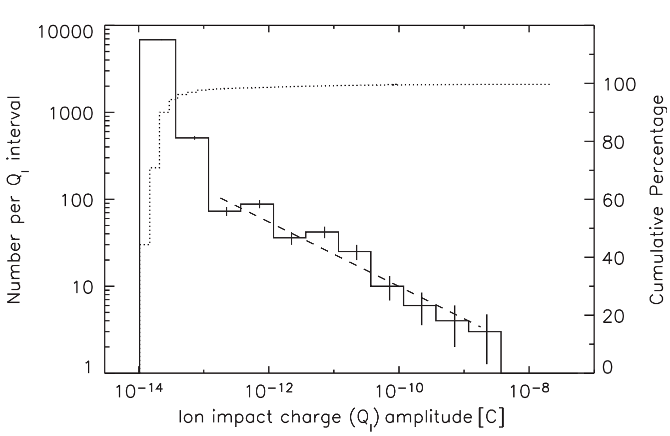

Fig. 5. Amplitude distribution of the impact charge Q_I for the 7625 dust particles detected in 1997–1999. The solid line indicates the number of impacts per charge interval, whereas the dotted line shows the cumulative distribution. Vertical bars indicate the $\sqrt{n}$ statistical fluctuation. A power law fit to the data with $Q_I > 10^{-13}$ C (big particles, AR2-6) is shown as a dashed line (Number $N \sim Q_I^{-0.37}$).

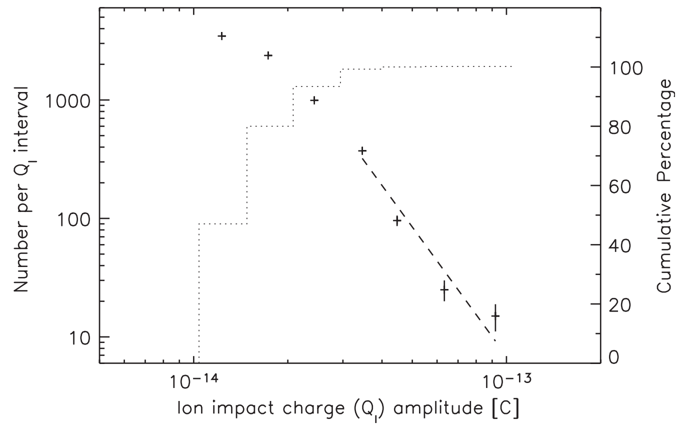

Fig. 6. Same as Fig. 5 but for the small particles in the lowest amplitude range (AR1) only. A power law fit to the data with 3×10^{-14} C $< Q_I < 10^{-13}$ C is shown as a dashed line (Number $N \sim Q_I^{-3.6}$).

The ratio of the channeltron charge Q_C and the ion collector charge Q_I is a measure of the channeltron amplification A which is an important parameter for dust impact identification (Paper I). The in-flight channeltron amplification was monitored in Papers II, IV, and VI for the initial seven years of the Galileo mission to identify possible degrading of the channeltron. The amplification $A = Q_C/Q_I$ for a channeltron high voltage setting of 1020 V (HV = 2) determined from impacts with 10^{-12} C $\leqslant Q_I \leqslant 10^{-10}$ C was in the range $1.4 \lesssim A \lesssim 1.8$. It did not indicate significant channeltron degradation until the end of 1996.

Here we repeat the same analysis for the 1997–1999 interval. Fig. 7 shows the charge ratio Q_C/Q_I as a function of Q_I for the same high voltage (HV = 2) as in the previous papers. The charge ratio Q_C/Q_I determined for 10^{-12} C $\leqslant Q_I \leqslant 10^{-10}$ C is $A \simeq 0.7$ (the data for each year individually give $A \simeq 1.0$ for 1997, 1.0 for 1998 and 0.2 for 1999, respectively). This is much lower than the earlier values, showing that significant channeltron degradation occurred. As a consequence, the channeltron voltage was raised two times (on days 99-305 and 99-345) to return to the original amplification factor. Details of the dust instrument degradation due to the harsh radiation environment in the jovian magnetosphere are described by Krüger et al. (2005, see also Section 2.5). It should be noted that the ratio Q_C/Q_I is entirely used for investigation of the instrument performance. It does not depend upon the properties of the detected particles.

Fig. 8 displays the calibrated masses and velocities of all 7625 dust grains detected in the 1997–1999 interval.

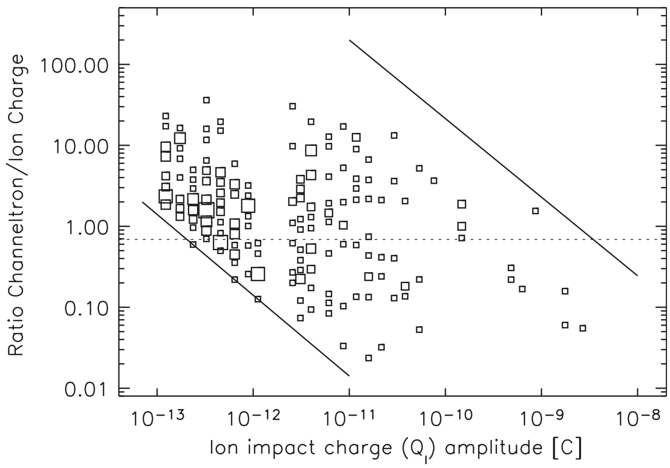

Fig. 7. Channeltron amplification factor $A = Q_C/Q_I$ as a function of impact charge Q_I for big particles (AR2-6) detected in 1997–1999. Only impacts measured with a channeltron high voltage setting HV = 2 are shown. The solid lines indicate the sensitivity threshold (lower left) and the saturation limit (upper right) of the channeltron. Squares indicate dust particle impacts, and the area of the squares is proportional to the number of events (the scaling of the squares is the same as in Paper VI). The dotted horizontal line shows the mean value of the channeltron amplification $A = 0.7$ calculated from 79 impacts in the ion impact charge range $10^{-12}\,C < Q_I < 10^{-10}\,C$.

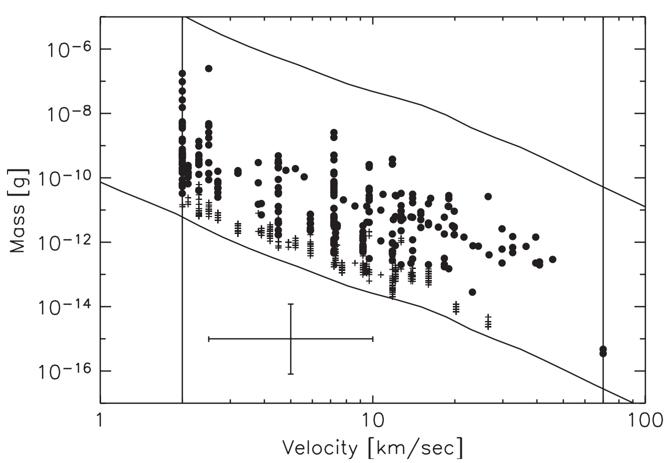

Fig. 8. Masses and impact speeds of all 7625 impacts recorded by DDS in 1997–1999. The lower and upper solid lines indicate the threshold and saturation limits of the detector, respectively, and the vertical lines indicate the calibrated velocity range. A sample error bar is shown that indicates a factor of 2 error for the velocity and a factor of 10 for the mass determination. Note that the small particles (plus signs) are most likely much faster and smaller than implied by this diagram (see text for details).

Impact velocities were measured over almost the entire calibrated range from 2 to $70\,km\,s^{-1}$, and the masses vary over 8 orders of magnitude from 10^{-7} g to 10^{-15} g. The mean errors are a factor of 2 for the velocity and a factor of 10 for the mass. Impact velocities below about $3\,km\,s^{-1}$ should be treated with caution. Anomalous impacts onto the sensor grids or structures other than the target generally lead to prolonged rise times of the charge signals. This in turn results in artificially low impact velocities and high dust particles masses.

The mass range populated by the particles is very similar to that reported for the 1996 measurements from the jovian system (Paper VI). However the largest and smallest masses are at the edges of the calibrated velocity range of DDS and, hence, they are the most uncertain. Any clustering of the velocity values is due to discrete steps in the rise time measurement but this quantization is much smaller than the velocity uncertainty. In addition, masses and velocities in the lowest amplitude range (AR1, particles indicated by plus signs) should be treated with caution. These are mostly jovian stream particles (Section 5.1) for which we have clear indications that their masses and velocities are outside the calibrated range of DDS (Zook et al., 1996, J.C. Liou, priv. comm.). The grains are probably much faster and smaller than implied by Fig. 8. On the other hand, the analysis of the dust clouds surrounding the Galilean moons has shown that the mass and velocity calibration is valid for the bigger particles (Krüger et al., 2000, 2003c). For many particles in the lowest two amplitude ranges (AR1 and AR2) the velocity had to be computed solely from the ion charge signal which leads to the striping in the lower mass range in Fig. 8 (most prominent above $10\,km\,s^{-1}$). In the higher amplitude ranges the velocity could normally be calculated as the geometric mean from both the target and the ion charge signals which leads to a more continuous distribution in the mass-velocity plane.

5. Discussion

5.1. Jovian dust streams dynamics

The majority of particles detected in the 1997–1999 interval considered here are tiny dust stream particles which almost exclusively populate amplitude range AR1 (Grün et al., 1998, see also Fig. 4). Frequency analysis of the 1996–1997 dust data showed that most of the grains originated from Jupiter's moon Io (Graps et al., 2000). The footprint of the Io torus found in the dust stream flux measurements also implied that Io behaves like a point source for the majority of the grains (Krüger et al., 2003b). The grains approach the sensor as collimated streams and their impact direction shows a characteristic behaviour that can only be explained by grains having a radius of about 10 nm and which strongly interact with the jovian magnetosphere (Grün et al., 1998). Strong magnetospheric interaction was also implied by prominent 5 and 10 h periodicities seen in the impact rate.

The impact direction of the stream particles in the 1997–1999 interval is shown in Figs. 9 and 10. On the inbound trajectory, when Galileo approached Jupiter, the grains were mainly detected from rotation angles $270^\circ \pm 70^\circ$. This is best seen in 1997 when we had continuous RTS data coverage from orbits G8 to E11.

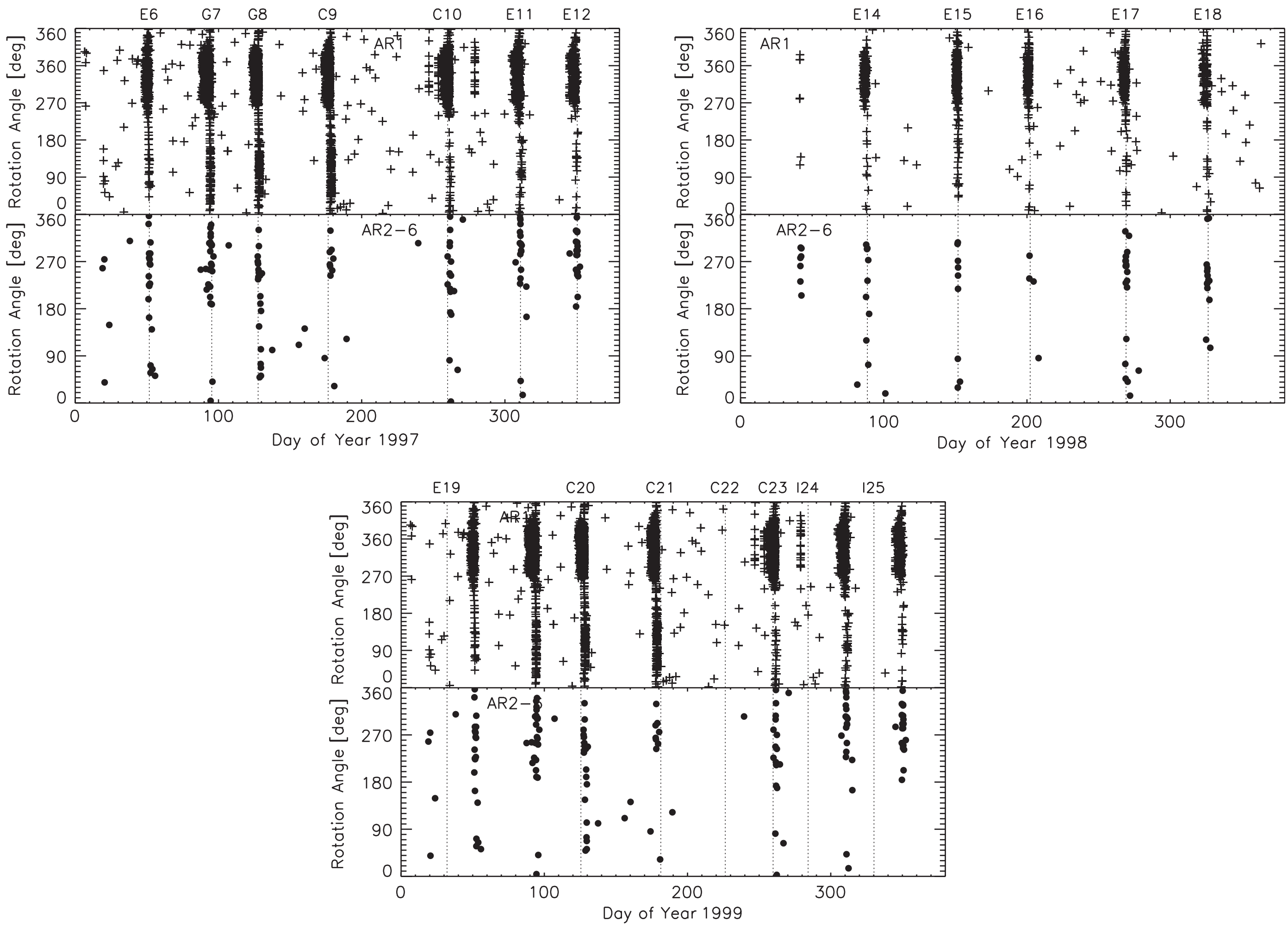

Fig. 9. Rotation angle vs. time for two different mass ranges, upper panel: small particles, AR1 (Io dust stream particles); lower panel: big particles, AR2-6. See Section 2 for an explanation of the rotation angle. The encounters with the Galilean moons are indicated by dotted lines.

One to two days before perijove passage of Galileo the impact direction shifted by 180° and the particles approached from $90^\circ \pm 70^\circ$. Rotation angles of 90° and 270° are close to the ecliptic plane. The dust detection geometry of DDS is displayed in Fig. 1.

The times of the onset, 180° shift and cessation of the dust streams as derived from the Galileo measurements are given in Table 4 and superimposed on the Galileo trajectory in Fig. 11. Reliable onset times could be determined for most revolutions of Galileo about Jupiter while the measurement of the 180° shift and cessation was prevented by spacecraft anomalies in a few cases. The times of the onset of stream particle impacts measured in classes 2 and 3 differed significantly from each other (not shown here), implying that different fields-of-view apply to stream particle impacts detected in both classes (Krüger et al., 1999b). We give the times of onset and cessation of the streams for class 3 only. Because of the reduced field-of-view for class 3 to only about 96° they can be better determined than those for class 2. Note that a reduced field-of-view for class 3 applies to the jovian stream particles (AR1) only.

In Fig. 12 we compare the measured times for the onset, 180° shift and cessation of the streams with values predicted from numerical modelling. Theoretical values were calculated from the numerically calculated trajectory of a 9 nm (radius) dust particle charged to an electric potential of +3 V which was released from an Io point source (Grün et al., 1998; Horányi et al., 1997). Times for the onset and cessation refer to the times when—in the simulation—these 'typical' grains approach the dust sensor at an angle of 108° w.r.t. the positive spin axis (cf. Fig. 1). This angle defines the edge of the DDS field-of-view for class 3 impacts in AR1 (Section 2.2).

It should be noted that the Horányi et al. (1997) model was developed and tested when dust data from only 2 Galileo orbits were available. With the data set covering four years of the mission we can test its validity during a much longer time period. Fig. 12 shows that within the estimated uncertainty most of the theoretically calculated

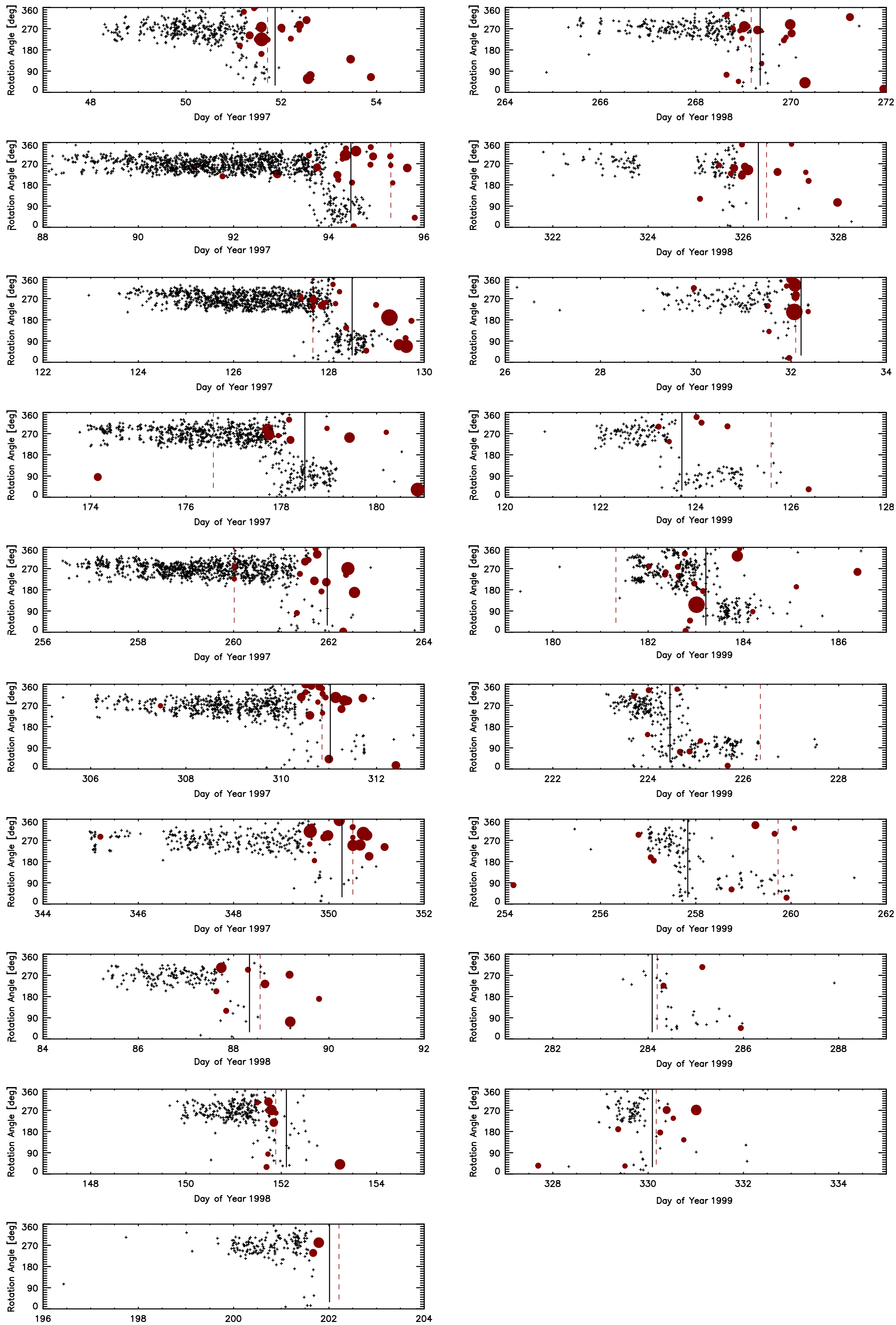

Fig. 10. Rotation angle detected by DDS in the inner jovian system in higher time resolution. Only dust data for classes 2 and 3 are shown. Crosses denote impacts in AR1, filled circles those in AR2-6. The size of the circles scales with the amplitude range. Dashed lines indicate perijove passages of Galileo, dotted lines closest approaches to the Galilean moons.

Table 4
Times of the onset (class 3), 180° shift and cessation (class 3) of the Jupiter dust streams

Orbit	Onset class 3	180° shift	Cessation class 3
E6	–	$97-051.4\pm0.2$	$97-051.7\pm0.7$
G7	$97-089.02\pm0.1$	$97-094.0\pm0.1$	$97-094.7\pm0.2$
G8	$97-124.40\pm0.2$	$97-127.9\pm0.1$	$97-128.7\pm0.1$
C9	$97-174.27\pm1.2$	$97-177.9\pm0.2$	$97-179.2\pm0.3$
C10	$97-257.14\pm0.5$	$97-261.3\pm0.3$	$97-262.1\pm0.8$
E11	$97-306.30\pm0.5$	$97-310.5\pm0.3$	$97-310.8\pm0.4$
E12	$97-346.84\pm0.2$	$97-349.7\pm0.2$	$97-351.0\pm0.8$
E14	$98-085.69\pm0.6$	$98-087.9\pm0.1$	$98-088.5\pm0.9$
E15	$98-149.99\pm0.4$	$98-151.9\pm0.1$	$98-152.3\pm0.6$
E16	$98-199.95\pm0.1$	–	–
E17	$98-266.92\pm0.1$	$98-269.2\pm0.1$	$98-269.2\pm1.0$
E18	$98-323.39\pm0.7$	–	–
E19	$99-029.83\pm0.7$	–	–
C20	$99-122.22\pm0.2$	$99-123.6\pm0.1$	$99-124.7\pm0.4$
C21	$99-181.52\pm0.2$	$99-183.3\pm0.2$	$99-184.0\pm0.4$
C22	$99-223.50\pm0.1$	$99-224.3\pm0.2$	$99-225.8\pm0.2$
C23	$99-257.02\pm0.2$	??	??
I24	–	$99-284.2\pm0.1$	$99-284.6\pm1.0$
I25	$99-328.97\pm0.5$	??	??

When no entries are given, either no RTS data were obtained (onset of E6) or a spacecraft anomaly prevented the collection of dust data. In cases where '??' are given, the number of detected particles was too low to reliably determine the time for the respective event.

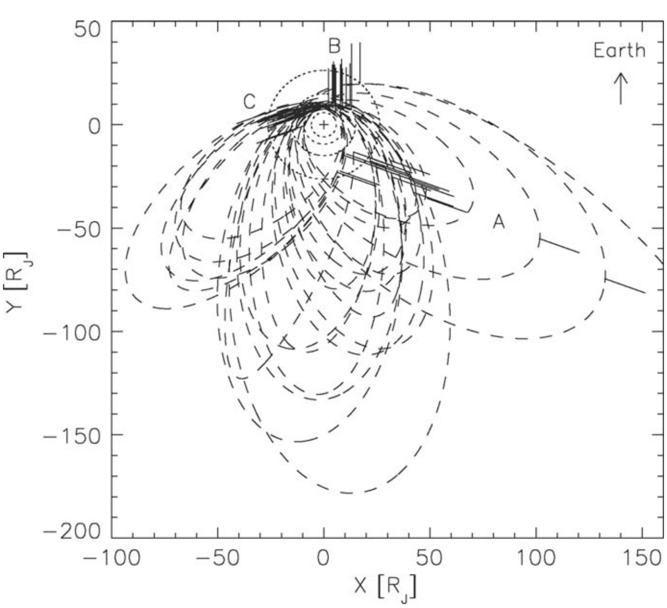

Fig. 11. Galileo trajectory in the jovian system from 1996 to 1999. The Y-axis points towards Earth. The impact directions of the grains at the time of onset (A), 180° shift (B) and cessation (C) of the dust streams are indicated. Note that the grains always move away from Jupiter.

times are compatible with the data. The mean deviations for the onset and cessation averaged over all orbits are $\overline{\Delta t_{\rm on}} = 0.04\pm0.38$ days and $\overline{\Delta t_{\rm off}} = -0.01\pm0.33$ days, respectively. Thus, on average the calculated theoretical trajectory very well reproduces the observed times $t_{\rm on}$ and

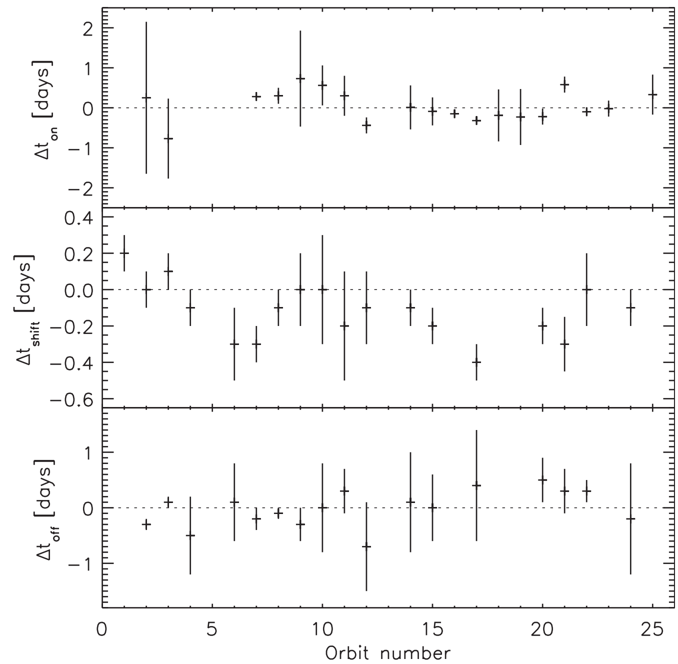

Fig. 12. Difference Δt between measured and theoretically predicted times of onset (top), 180° shift (middle) and cessation (bottom) of the dust stream impacts (class 3) for 1996–1999. Theoretical times were derived for a 9 nm dust particle charged to +3 V which was released from an Io source (Grün et al., 1998).

$t_{\rm off}$. However, for the shift time the average is $\overline{\Delta t_{\rm shift}} = -0.12\pm0.15$ days, indicating that there is a residual in the reproduction of the shift time by the modelling. However, the individual shift times of the streams are more difficult to determine than the times for onset and cessation. Overall, the agreement between the measured data and the theoretical predictions indicates that our selected 9 nm grain gives good agreement with the measurements, confirming earlier results (Horányi et al., 1997). In particular, for bigger dust grains moving on Keplerian orbits the agreement would be much worse (Thiessenhusen et al., 2000, see also Fig. 10). Note that outside the region of the Galilean moons the calculated grain impact speeds onto the dust detector exceed 300 km s^{-1} and their terminal speeds reached when leaving the jovian magnetosphere are about 350 km s^{-1}.

5.2. Mass distribution of "big" particles in the jovian system

During each revolution about Jupiter, Galileo recorded several impacts of dust particles in amplitude ranges AR2-6. The majority of these impacts occurred in the inner jovian system in the region between the Galilean moons (Fig. 10). The geometric behaviour of these detections differed significantly from that of the stream particles recorded in AR1. Most notably, a shift in impact direction occurred significantly later than for the stream particles, implying different orbital characteristics of the grains. The majority of the grains form a dust ring between the Galilean moons (Krivov and Banaszkiewicz, 2001; Krivov et al., 2002a,b). Two groups of grains can be distinguished in the ring: particles on bound prograde or retrograde orbits about Jupiter, respectively. Analysis of the 1996–1999 Galileo data showed that the number density of the prograde population exceeds that of the retrograde ones by at least a factor of four (Thiessenhusen et al., 2000). A fraction of these grains may be interplanetary or interstellar grains captured by the jovian magnetosphere (Colwell et al., 1998a,b). The prograde population in the ring is fed by particles escaping from impact-generated dust clouds surrounding the Galilean moons (Krivov et al., 2002a).

Another potential source for big dust grains is dust released by comet Shoemaker-Levy 9 during its tidal disruption in 1992. A fraction of the debris was predicted to form a dust ring in the inner jovian system roughly inside Europa's orbit within 10 years after the fragmentation of the comet nucleus (Horányi, 1994). Radii of the debris particles in this ring were predicted to be about 2 μm, and the grains should predominantly fall on retrograde orbits. The expected optical depth was $10^{-8} < \tau < 10^{-6}$. It implies that this ring should be detectable with ground-based and Galileo imaging. However, it did not show up on recent Galileo images (D.P. Hamilton, priv. comm.) which were sensitive to $\tau \simeq 10^{-8}$, indicating that the dust densities must be lower than expected from theory.

The segregation of the debris particles from comet Shoemaker-Levy 9 during the last decade should have lead to a temporal variation of the dust density within and around Europa's orbit. Such a temporal variation, however, could not be clearly identified in the Galileo dust data set yet (A.V. Krivov, priv. comm.). Temporal variations turned out to be very difficult to identify because of several long-term effects: the changing detection geometry of the dust instrument over time and the aging-related changes of the instrument sensitivity must be corrected. In addition, the possibility of true spatial variations, like, for example, a displacement of the jovian dust ring—predicted by dynamical models (Krivov et al., 2002a)—further complicates the analysis.

With the entire 1996–1999 data set we have a sufficiently large number of impacts (370) to construct a statistically meaningful mass distribution of these "big" grains. Ground calibration and the analysis of the Galilean dust clouds (Krüger et al., 2000, 2003c) showed that the instrument calibration gives reliable impact speeds up to at least $10\,\mathrm{km\,s^{-1}}$. If we assume that the grains move on prograde jovicentric Keplerian orbits, the particles detected in AR2-6 are expected to have impact speeds in this range so that we can also apply the calibration to these grains. The mass and speed calibration can be applied to data until the end of 1999, while for later measurements it becomes useless because the electronics degradation of DDS lead to significant shifts in the measured charge amplitudes and rise times (Krüger et al., 2005).

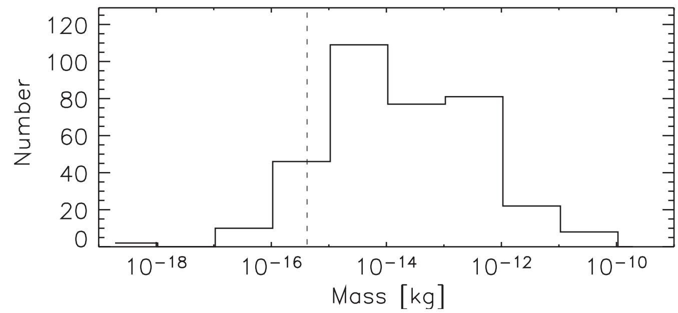

Fig. 13. Mass distribution of particles detected in 1996–1999 in AR2-6 ("big" particles) derived from the instrument calibration. No correction for electronics degradation was applied (Krüger et al., 2005). The vertical dotted line indicates the lower bound of AR2 for an impact speed of $10\,\mathrm{km\,s^{-1}}$.

The mass distribution for the "big" particles detected in AR2-6 is shown in Fig. 13. The average mass is 3×10^{-14} kg, which, for spherical grains with density $1\,\mathrm{g\,cm^{-3}}$, corresponds to a particle radius of about 2 μm. We therefore call these grains "big" particles to distinguish them from the tiny stream particles which have two orders of magnitude smaller radii. Note that the size distribution strongly increases towards smaller grains. On the other hand, the biggest detected particles have radii of about 10 μm. The lower bound for detection in AR2 for $10\,\mathrm{km\,s^{-1}}$ is only indicative of particles on circular uninclined jovicentric orbits. Their true impact speeds almost certainly had a very large variation (Thiessenhusen et al., 2000).

6. Summary

In this paper, which is the eighth in a series of Galileo and Ulysses papers, we present data from the Galileo dust instrument for the period January 1997–December 1999. In this time interval the spacecraft completed 21 revolutions about Jupiter in the jovicentric distance range between 6 and $150 R_J$ (Jupiter radius, $R_J = 71,492$ km).

The data sets of a total of 7625 (or 3% of the total) recorded dust impacts were transmitted to Earth in this period. Many more impacts (97%) were counted with the accumulators of the instrument but their complete information was lost because of the low data transmission capability of the Galileo spacecraft. Together with 8236 impacts recorded in interplanetary space and in the Jupiter system between Galileo's launch in October 1989 and December 1996 published earlier (Grün et al., 1995a; Krüger et al., 1999a, 2001a), the complete data set of dust impacts measured with the Galileo dust detector between launch and the end of 1999 contains 15861 impacts.

Galileo has been an extremely successful dust detector, measuring dust streams flowing away from Jupiter, dust escaping from the Galilean moons and a tenuous dust ring throughout the jovian magnetosphere continuously over the three year timespan of data considered in this paper.

Most of the time the jovian dust streams dominated the overall impact rate, reaching maxima of more than 10 impacts per minute in the inner jovian system in the region between the Galilean moons. More than 100 impacts per minute were recorded on 1 July 1999 (day 99-182). It was one of the periods with the highest dust impact rates recorded during the entire Galileo Jupiter mission (Krüger et al., 2003a). The measured times of onset, cessation and a 180° shift in the impact direction of the stream particles measured during most of Galileo's revolutions about Jupiter in the 1996–1999 interval are very well reproduced by the trajectories of 9 nm (radius) dust grains charged to +3 V obtained in numerical simulations, confirming earlier results (Horányi et al., 1997; Grün et al., 1998). These times differ significantly from those expected for grains moving on bound Keplerian orbits, consistent with strong interaction of the tiny stream particles with the jovian magnetic field. It should be noted that these grains are smaller and faster than the calibrated range of the dust instrument (Zook et al., 1996).

In the 1996–1999 interval bigger micron-sized dust grains were mostly detected in the inner jovian system in the region between the Galilean moons. They separate into two populations, one moving on prograde jovicentric orbits and the other one moving on retrograde orbits (Colwell et al., 1998b). The 1996–1999 Galileo dust data showed that the number density of the prograde population exceeds that of the retrograde ones by at least a factor of four (Thiessenhusen et al., 2000). In this paper we have constructed the size distribution for these grains. The average radius of 370 measured grains is about 2 μm and the size distribution strongly rises towards smaller grains. The largest grains detected are about 10 μm (assuming spherical grains with density $1\,\mathrm{g\,cm^{-3}}$). An additional contribution of dust debris released during the tidal disruption of comet Shoemaker-Levy 9 in 1992 was predicted to exist (Horányi, 1994) but has not been identified in the Galileo dust data set.

Finally, Galileo detected tenuous clouds of dust grains within the Hill spheres of all four Galilean moons. The 1996–1999 Galileo dust data set was used for the analysis of these clouds in earlier publications (e.g. Krüger et al., 2003c). The dust clouds are formed by secondary ejecta grains kicked up from the moons' surfaces (Krivov et al., 2003). Detected particle sizes were ~0.3–1 μm, and the measured grain size distributions agreed very well with expectations from laboratory impact experiments.

Strong degradation of the dust instrument electronics was recognised in the data (Krüger et al., 2005) which was most likely caused by the harsh radiation environment in the jovian magnetosphere. It caused a reduced instrument sensitivity for noise and dust detection during the Galileo mission. A reduced amplification of the channeltron was counterbalanced by two increases in the channeltron high voltage in 1999 to maintain stable instrument operation. The Galileo data set obtained until the end of 1999 is not seriously affected by this degradation. In particular, no correction for dust fluxes, grain speeds and masses are necessary and results obtained with this data set in earlier publications remain valid. Also, the Galileo dust data published in earlier papers in this series (Papers II, IV and VI) remain unchanged. It should be noted, however, that dust fluxes calculated with a sensitive area taking into account only the sensor target overestimate the true dust fluxes and number densities by about 20% because the inner sensor side walls turned out to be as sensitive to dust impacts as the sensor target itself (Altobelli et al., 2004; Willis et al., 2005). The dust data set from 2000 until the end of the Galileo mission in 2003 will be the subject of a forthcoming paper in this series of Galileo and Ulysses dust data papers.

Acknowledgements

The authors wish to thank the Galileo project at NASA/JPL for effective and successful mission operations. This research was supported by the German Bundesministerium für Bildung und Forschung through Deutsches Zentrum für Luft- und Raumfahrt e.V. (DLR, grant 50 QJ 95033). Support by MPI für Kernphysik and MPI für Sonnensystemforschung is also gratefully acknowledged.

References

Altobelli, N., Moissl, R., Krüger, H., Landgraf, M., Grün, E., 2004. Influence of wall impacts on the Ulysses dust detector in modelling the interstellar dust flux. Planetary Space Sci. 52, 1287–1295.

Colwell, J.E., Horányi, M., Grün, E., 1998a. Jupiter's exogenic dust ring. J. Geophys. Res. 103, 20023–20030.

Colwell, J.E., Horányi, M., Grün, E., 1998b. Capture of interplanetary and interstellar dust by the Jovian magnetosphere. Science 280, 88–91.

D'Amario, L.A., Bright, L.E., Wolf, A.A., 1992. Galileo trajectory design. Space Sci. Rev. 60, 23–78.

Flandes, A., 2005. Dust dynamics in the jovian system. Ph.D. Thesis, Universidad Nacional Autonoma de Mexico.

Graps, A.L., 2001. Io revealed in the Jovian dust streams. Ph.D. Thesis, Ruprecht-Karls-Universität Heidelberg.

Graps, A.L., Grün, E., Svedhem, H., Krüger, H., Horányi, M., Heck, A., Lammers, S., 2000. Io as a source of the Jovian dust streams. Nature 405, 48–50.

Grün, E., Fechtig, H., Hanner, M.S., Kissel, J., Lindblad, B.A., Linkert, D., Maas, D., Morfill, G.E., Zook, H.A., 1992a. The Galileo dust detector. Space Sci. Rev. 60, 317–340.

Grün, E., Fechtig, H., Kissel, J., Linkert, D., Maas, D., McDonnell, J.A.M., Morfill, G.E., Schwehm, G.H., Zook, H.A., Giese, R.H., 1992b. The Ulysses dust experiment. Astronomy Astrophys. 92 (Suppl.), 411–423.

Grün, E., Zook, H.A., Baguhl, M., Balogh, A., Bame, S.J., Fechtig, H., Forsyth, R., Hanner, M.S., Horányi, M., Kissel, J., Lindblad, B.A., Linkert, D., Linkert, G., Mann, I., McDonnell, J.A.M., Morfill, G.E., Phillips, J.L., Polanskey, C., Schwehm, G.H., Siddique, N., Staubach, P., Svestka, J., Taylor, A., 1993. Discovery of Jovian dust streams and interstellar grains by the Ulysses spacecraft. Nature 362, 428–430.

Grün, E., Baguhl, M., Divine, N., Fechtig, H., Hamilton, D.P., Hanner, M.S., Kissel, J., Lindblad, B.A., Linkert, D., Linkert, G., Mann, I., McDonnell, J.A.M., Morfill, G.E., Polanskey, C., Riemann, R., Schwehm, G.H., Siddique, N., Staubach, P., Zook, H.A., 1995a. Three years of Galileo dust data. Planetary Space Sci. 43, 953–969 (Paper II).

Grün, E., Baguhl, M., Divine, N., Fechtig, H., Hamilton, D.P., Hanner, M.S., Kissel, J., Lindblad, B.A., Linkert, D., Linkert, G., Mann, I., McDonnell, J.A.M., Morfill, G.E., Polanskey, C., Riemann, R., Schwehm, G.H., Siddique, N., Staubach, P., Zook, H.A., 1995b. Two years of Ulysses dust data. Planetary Space Sci. 43, 971–999 (Paper III).

Grün, E., Baguhl, M., Hamilton, D.P., Kissel, J., Linkert, D., Linkert, G., Riemann, R., 1995c. Reduction of Galileo and Ulysses dust data. Planetary Space Sci. 43, 941–951 (Paper I).

Grün, E., Baguhl, M., Hamilton, D.P., Riemann, R., Zook, H.A., Dermott, S.F., Fechtig, H., Gustafson, B.A., Hanner, M.S., Horányi, M., Khurana, K.K., Kissel, J., Kivelson, M., Lindblad, B.A., Linkert, D., Linkert, G., Mann, I., McDonnell, J.A.M., Morfill, G.E., Polanskey, C., Schwehm, G.H., Srama, R., 1996a. Constraints from Galileo observations on the origin of Jovian dust streams. Nature 381, 395–398.

Grün, E., Hamilton, D.P., Riemann, R., Dermott, S.F., Fechtig, H., Gustafson, B.A., Hanner, M.S., Heck, A., Horányi, M., Kissel, J., Kivelson, M., Krüger, H., Lindblad, B.A., Linkert, D., Linkert, G., Mann, I., McDonnell, J.A.M., Morfill, G.E., Polanskey, C., Schwehm, G.H., Srama, R., Zook, H.A., 1996b. Dust measurements during Galileo's approach to Jupiter and Io encounter. Science 274, 399–401.

Grün, E., Krüger, P., Dermott, S.F., Fechtig, H., Graps, A.L., Gustafson, B.A., Hamilton, D.P., Heck, A., Horányi, M., Kissel, J., Lindblad, B.A., Linkert, D., Linkert, G., Mann, I., McDonnell, J.A.M., Morfill, G.E., Polanskey, C., Schwehm, G.H., Srama, R., Zook, H.A., 1997. Dust measurements in the Jovian magnetosphere. Geophys. Res. Lett. 24, 2171–2174.

Grün, E., Krüger, H., Graps, A., Hamilton, D.P., Heck, A., Linkert, G., Zook, H., Dermott, S.F., Fechtig, H., Gustafson, B., Hanner, M., Horányi, M., Kissel, J., Lindblad, B., Linkert, G., Mann, I., McDonnell, J.A.M., Morfill, G.E., Polanskey, C., Schwehm, G.H., Srama, R., 1998. Galileo observes electromagnetically coupled dust in the Jovian magnetosphere. J. Geophys. Res. 103, 20011–20022.

Heck, A., 1998. Modellierung und Analyse der von der Raumsonde Galileo im Jupitersystem vorgefundenen Mikrometeoroiden-Populationen. Ph.D. Thesis, Ruprecht-Karls-Universität Heidelberg.

Horányi, M., 1994. New Jovian ring? Geophys. Res. Lett. 21, 1039–1042.

Horányi, M., Grün, E., Heck, A., 1997. Modeling the Galileo dust measurements at Jupiter. Geophys. Res. Lett. 24, 2175–2178.

Johnson, T.V., Yeates, C., Young, R., 1992. Galileo Mission Overview. Space Sci. Rev. 60, 3–21.

Kempf, S., Srama, R., Altobelli, N., Auer, S., Tschernjawski, V., Bradley, J., Burton, M.E., Helfert, S., Johnson, T.V., Krüger, H., Moragas-Klostermeyer, G., Grün, E., 2004. Cassini between Earth and asteroid belt: first in situ charge measurements of interplanetary grains. Icarus 171, 317–335.

Krivov, A.V., Banaszkiewicz, H., 2001. Unusual origin, evolution and fate of icy ejecta from Hyperion. Planetary Space Sci. 49, 1265–1279.

Krivov, A.V., Krüger, H., Grün, E., Thiessenhusen, K.-U., Hamilton, D.P., 2002a. A tenuous dust ring of Jupiter formed by escaping ejecta from the Galilean satellites. J. Geophys. Res. 107, E1, 10.1029/2000JE001434.

Krivov, A.V., Wardinski, I., Spahn, F., Krüger, H., Grün, E., 2002b. Dust on the outskirts of the Jovian system. Icarus 157, 436–455.

Krivov, A.V., Sremčević, M., Spahn, F., Dikarev, V.V., Kholshevnikov, K.V., 2003. Impact-generated dust clouds around planetary satellites: spherically-symmetric case. Planetary Space Sci. 51, 251–269.

Krüger, H., 2003. Jupiter's Dust Disc, An Astrophysical Laboratory, Shaker Verlag, Aachen, ISBN 3-8322-2224-3, Habilitation Thesis Ruprecht-Karls-Universität Heidelberg.

Krüger, H., Grün, E., Hamilton, D.P., Baguhl, M., Dermott, S.F., Fechtig, H., Gustafson, B.A., Hanner, M.S., Horányi, M., Kissel, J., Lindblad, B.A., Linkert, D., Linkert, G., Mann, I., McDonnell, J.A.M., Morfill, G.E., Polanskey, C., Riemann, R., Schwehm, G.H., Srama, R., Zook, H.A., 1999a. Three years of Galileo dust data: II. 1993 to 1995. Planetary Space Sci. 47, 85–106 (Paper IV).

Krüger, H., Grün, E., Heck, A., Lammers, S., 1999b. Analysis of the sensor characteristics of the Galileo dust detector with collimated Jovian dust stream particles. Planetary Space Sci. 47, 1015–1028.

Krüger, H., Grün, E., Landgraf, M., Baguhl, M., Dermott, S.F., Fechtig, H., Gustafson, B.A., Hamilton, D.P., Hanner, M.S., Horányi, M., Kissel, J., Lindblad, B., Linkert, D., Linkert, G., Mann, I., McDonnell, J.A.M., Morfill, G.E., Polanskey, C., Schwehm, G.H., Srama, R., Zook, H.A., 1999c. Three years of Ulysses dust data: 1993 to 1995. Planetary Space Sci. 47, 363–383 (Paper V).

Krüger, H., Krivov, A.V., Hamilton, D.P., Grün, E., 1999d. Detection of an impact-generated dust cloud around Ganymede. Nature 399, 558–560.

Krüger, H., Krivov, A.V., Grün, E., 2000. A dust cloud of Ganymede maintained by hypervelocity impacts of interplanetary micrometeoroids. Planetary Space Sci. 48, 1457–1471.

Krüger, H., Grün, E., Graps, A.L., Bindschadler, D.L., Dermott, S.F., Fechtig, H., Gustafson, B.A., Hamilton, D.P., Hanner, M.S., Horányi, M., Kissel, J., Lindblad, B., Linkert, D., Linkert, G., Mann, I., McDonnell, J.A.M., Morfill, G.E., Polanskey, C., Schwehm, G.H., Srama, R., Zook, H.A., 2001a. One year of Galileo dust data from the jovian system: 1996. Planetary Space Sci. 49, 1285–1301 (Paper VI).

Krüger, H., Grün, E., Landgraf, M., Dermott, S.F., Fechtig, H., Gustafson, B.A., Hamilton, D.P., Hanner, M.S., Horányi, M., Kissel, J., Lindblad, B., Linkert, D., Linkert, G., Mann, I., McDonnell, J.A.M., Morfill, G.E., Polanskey, C., Schwehm, G.H., Srama, R., Zook, H.A., 2001b. Four years of Ulysses dust data: 1996 to 1999. Planetary Space Sci. 49, 1303–1324 (Paper VII).

Krüger, H., Geissler, P., Horányi, M., Graps, A.L., Kempf, S., Srama, R., Moragas-Klostermeyer, G., Moissl, R., Johnson, T.V., Grün, E., 2003a. Jovian dust streams: A monitor of Io's volcanic plume activity. Geophys. Res. Lett. 30, 2101–2105.

Krüger, H., Horányi, M., Grün, E., 2003b. Jovian dust streams: probes of the Io plasma torus. Geophys. Res. Lett. 30, 1058–1061.

Krüger, H., Krivov, A.V., Sremčević, M., Grün, E., 2003c. Galileo measurements of impact-generated dust clouds surrounding the Galilean satellites. Icarus 164, 170–187.

Krüger, H., Horányi, M., Krivov, A.V., Graps, A.L., 2004. Jovian dust: streams, clouds and rings. In: Fran Bagenal, Timothy E. Dowling, William B. McKinnon (Eds.), Jupiter. The Planet, Satellites and Magnetosphere, Cambridge planetary science, vol. 1, Cambridge University Press, Cambridge, UK, pp. 219–240 ISBN 0-521-81808-7.

Krüger, H., Grün, E., Linkert, D., Linkert, G., Moissl, R., 2005. Galileo long-term dust monitoring in the jovian magnetosphere. Planetary Space Sci. 53, 1109–1120.

Krüger, H., Altobelli, N., Anweiler, B., Dermott, S.F., Dikarev, V., Fechtig, H., Graps, A.L., Grün, E., Gustafson, B.A., Hamilton, D.P., Hanner, M.S., Horányi, M., Kissel, J., Landgraf, M., Lindblad, B., Linkert, D., Linkert, G., Mann, I., McDonnell, J.A.M., Morfill, G.E., Polanskey, C., Schwehm, G.H., Srama, R., Zook, H.A., 2006. Five years of Ulysses dust data: 2000 to 2004. Planetary Space Sci. (Paper IX), in press, doi:10.1016/j.pss.2006.04.015.

Moissl, R., 2005. Galileo's Staubmessungen in Jupiters Gossamer-Ringen, Ruprecht-Karls-Universität Heidelberg, Diplom thesis.

Postberg, F., Kempf, S., Green, S.F., Hillier, J.K., McBride, N., Grün, E., 2006. Composition of jovian dust stream particles. Icarus, in press.

Sremčević, M., Krivov, A.V., Spahn, F., 2003. Impact-generated dust clouds around planetary satellites: asymmetry effects. Planetary Space Sci. 51, 455–471.

Sremčević, M., Krivov, A.V., Krüger, H., Spahn, F., 2005. Impact-generated dust clouds around planetary satellites: model versus Galileo data. Planetary Space Sci. 53, 625–641.

Svestka, J., Auer, S., Baguhl, M., Grün, E., 1996. In: Gustafson, B.A., Hanner, M.S. (Eds.), Physics, Chemistry and Dynamics of Interplanetary Dust, ASP Conference Series, vol. 104, pp. 481–484.

Thiessenhusen, K.-U., Krüger, H., Spahn, F., Grün, E., 2000. Dust grains around Jupiter—the observations of the Galileo dust detector. Icarus 144, 89–98.
Willis, M.J., Burchell, M., Cole, M., McDonnell, J.A.M., 2004. Influence of impact ionization detection methods on determination of dust particle flux in space. Planetary Space Sci. 52, 711–725.
Willis, M.J., Burchell, M., Ahrens, T.J., Krüger, H., Grün, E., 2005. Decreased values of cosmic dust number density estimates in the Solar system. Icarus 176, 440–452.
Zook, H.A., Grün, E., Baguhl, M., Hamilton, D.P., Linkert, G., Linkert, D., Liou, J.-C., Forsyth, R., Phillips, J.L., 1996. Solar wind magnetic field bending of Jovian dust trajectories. Science 274, 1501–1503.